

**Zeitschrift:** Schweizerische mineralogische und petrographische Mitteilungen =  
Bulletin suisse de minéralogie et pétrographie

**Band:** 78 (1998)

**Heft:** 2

**Artikel:** Mineral parageneses in the Piampaludo eclogitic body, Gruppo di Voltri,  
Western Ligurian Alps

**Autor:** Liou, Juhn G. / Zhang, Ruyuan / Ernst, W.G.

**DOI:** <https://doi.org/10.5169/seals-59291>

### **Nutzungsbedingungen**

Die ETH-Bibliothek ist die Anbieterin der digitalisierten Zeitschriften auf E-Periodica. Sie besitzt keine Urheberrechte an den Zeitschriften und ist nicht verantwortlich für deren Inhalte. Die Rechte liegen in der Regel bei den Herausgebern beziehungsweise den externen Rechteinhabern. Das Veröffentlichen von Bildern in Print- und Online-Publikationen sowie auf Social Media-Kanälen oder Webseiten ist nur mit vorheriger Genehmigung der Rechteinhaber erlaubt. [Mehr erfahren](#)

### **Conditions d'utilisation**

L'ETH Library est le fournisseur des revues numérisées. Elle ne détient aucun droit d'auteur sur les revues et n'est pas responsable de leur contenu. En règle générale, les droits sont détenus par les éditeurs ou les détenteurs de droits externes. La reproduction d'images dans des publications imprimées ou en ligne ainsi que sur des canaux de médias sociaux ou des sites web n'est autorisée qu'avec l'accord préalable des détenteurs des droits. [En savoir plus](#)

### **Terms of use**

The ETH Library is the provider of the digitised journals. It does not own any copyrights to the journals and is not responsible for their content. The rights usually lie with the publishers or the external rights holders. Publishing images in print and online publications, as well as on social media channels or websites, is only permitted with the prior consent of the rights holders. [Find out more](#)

**Download PDF:** 30.04.2026

**ETH-Bibliothek Zürich, E-Periodica, <https://www.e-periodica.ch>**

## Mineral parageneses in the Piampaludo eclogitic body, Gruppo di Voltri, Western Ligurian Alps

by Juhn G. Liou<sup>1</sup>, Ruyuan Zhang<sup>1</sup>, W.G. Ernst<sup>1</sup>, Jun Liu<sup>1</sup> and Roger McLimans<sup>2</sup>

### Abstract

Long-duration piston-cylinder phase-equilibrium experiments in the basalt-H<sub>2</sub>O system at 600–950 °C, 0.8–3.0 GPa demonstrate that amphibolite transforms to eclogite with increasing pressure by three reversed reactions: appearance of garnet, breakdown of plagioclase, and decomposition of amphibole. The garnet-in, plagioclase-out, and amphibole-out phase boundaries, coupled with the presence of titanium-rich phases, divide P-T space into four regions corresponding to the amphibolite, garnet amphibolite, hornblende-eclogite, and eclogite facies. For MORB bulk-rock compositions, rutile occupies a broad P-T synthesis field at high pressures, titanite occurs at low P and T, and ilmenite is confined to low P and high T.

At Piampaludo in the Western Ligurian Alps, an eclogitic ferrogabbro layer at least 120 m thick is encased in the Beigua antigoritic serpentinite. The eclogitic core is massive, relatively unaltered, and homogeneous, whereas the margin of the body is strongly foliated and retrograded. The TiO<sub>2</sub> content of the eclogite averages 6%, dominantly as rutile, but massive eclogite seems to be richer in rutile than the foliated margins. Omphacite + garnet + rutile rocks are differentiated Fe–Ti rich gabbros metamorphosed to eclogitic assemblages, followed by amphibolite/blueschist- and later greenschist-facies overprinting. Titanium resides principally in rutile, ilmenite is common, and titanite is locally significant. Rutile is rimmed by ilmenite; cracks within garnet contain ilmenite, albite, and chlorite. Titanite is the latest Ti phase, forming after ilmenite and rutile. Rutile exhibits different colors and modes of occurrence, but it is remarkably homogeneous, containing minor FeO (0.23–0.61 wt%), MnO (0.0–0.49 wt%), and CaO (0.0–0.46). In contrast, ilmenite shows marked compositional variations, with MnO (0.31–5.73 wt%), MgO (0.17–0.69 wt%), CaO (0.0–0.48 wt%), and detectable ZnO. Titanites contain 0.78–1.32 wt% Al<sub>2</sub>O<sub>3</sub> and 0.22–0.57 wt% FeO. The occurrence of garnet + omphacite ± talc + rutile as the main eclogite assemblage suggests high-pressure (> 1.5 GPa) metamorphism, but garnet-clinopyroxene geothermometers indicate recrystallization at only 425 ± 75 °C. Because the eclogitic rocks contain abundant zoned amphiboles and widespread retrograde assemblages, garnet and clinopyroxene probably partly re-equilibrated during the amphibolite/blueschist-facies overprint, which might explain the low-temperature estimates.

*Keywords:* Fe+Ti-rich metagabbro, eclogite, rutile, HP parageneses, phase relations, Ligurian Alps.

### Introduction

Common eclogitic silicates do not contain measurable titanium; the only important Ti-bearing mineral is rutile. Accordingly, high-P metamorphism is a natural lithologic process which concentrates TiO<sub>2</sub> into a mechanically separable phase – rutile, a commodity of considerable value to the pigment industry. Unfortunately, during ascent of eclogitic rocks from great depths, original phase assemblages are subjected to retrogression.

Rutile is commonly replaced, first by ilmenite and later by titanite; ilmenite is the dominant Ti-bearing phase in strongly retrograded and foliated eclogites. These secondary phases are of much less utility as a commercial source of TiO<sub>2</sub>. Hence, study of the paragenesis of Ti-bearing phases provides a useful indicator in the search for and exploitation of Ti-ore in eclogitic rocks (FORCE, 1991).

The goals of this petrologic study of Gruppo di Voltri rutile-bearing eclogitic samples from NW

<sup>1</sup> Dept. of Geological and Environmental Sciences, Stanford University, Stanford, CA 94305, USA.  
<liou@pangea.stanford.edu>

<sup>2</sup> E.I. Du Pont de Nemours & Co., Deepwater, NJ 08023, USA.

Italy, which integrates experimental phase-equilibrium data published by LIU et al. (1996) and ERNST and LIU (in press), are: (1) to characterize modal compositions of both rutile-rich and rutile-poor samples, and to correlate them with XRF data in order to evaluate the nature of the protoliths; (2) to identify modes of occurrence and chemical variations of rutile and associated Ti-bearing phases; (3) to compare experimentally derived phase relations with occurrences of rutile, ilmenite, and titanite in order to evaluate potential rutile ores as a prospecting tool; (4) to determine the paragenesis and compositions of associated silicates in order to quantify the episodes of metamorphic recrystallization and P-T conditions of formation; and (5) to elucidate mechanisms and chemical reactions leading to the genesis and concentration of rutile during high-P metamorphism. Attainment of these goals should contribute to a better understanding of the petrogenesis of Ti-rich ores, aiding exploration and exploitation of such deposits in other high-pressure areas as well as NW Italy.

#### Experimental phase-equilibrium investigation of MORB + H<sub>2</sub>O

Results of long-run-duration piston-cylinder experiments (up to 30 days at 700 °C, and 90 days at 600 °C) on fresh, glassy oceanic tholeiite were presented by LIU et al. (1996) and ERNST and LIU (in press). The P-T range covered was 600–950 °C, 0.8–3.0 GPa. Compositions of the starting materials, unzoned synthesized phases, run data, and demonstration of reaction reversal were detailed in these papers, suggesting a close approach to chemical equilibrium. While the results of LIU et al. and ERNST and LIU are generally compatible with experimental phase relations produced by previous workers (ESSENE et al., 1970; HELZ, 1973, 1979; LIOU et al., 1974; SPEAR, 1981; MOODY et al., 1983; POLI, 1993 and POLI and SCHMIDT, 1997), some of these early studies did not demonstrate reaction reversal, or did not document homogeneous phase compositions.

With increasing pressure, basaltic amphibolite transforms to an eclogite-facies assemblage by three sliding equilibria, as shown in figure 1: these involve the appearance of garnet, breakdown of plagioclase, and decomposition of amphibole. The three multivariant reaction boundaries divide P-T space into four regions, corresponding to the amphibolite, garnet amphibolite, hornblende-eclogite, and eclogite facies. The solidus of the system is located between 700–750 °C at 1.0–2.2 GPa. Mineral assemblages (plus a Ti-rich phase) of the

four P-T regions are Pl + Hb + Qtz, Grt + Pl + Hb + Qtz, Grt + Hb ± Cpx + Qtz, and Grt + Cpx + Qtz/Coe at  $T \leq 700$  °C, respectively; and Pl + Hb ± Cpx + melt, Grt + Hb ± Cpx + melt, Grt + Hb + Cpx, and Grt + Cpx + melt at  $T \geq 750$  °C, respectively. (Mineral abbreviations used in this paper are after KRETZ, 1983.)

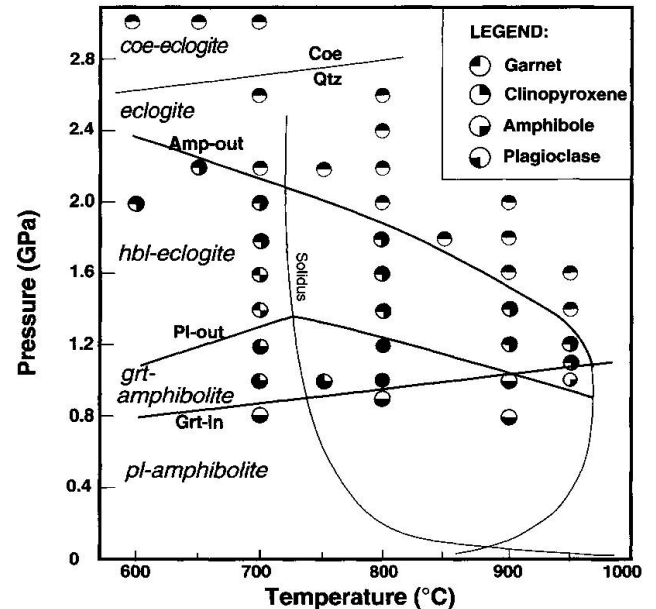


Fig. 1 Experimentally determined phase relations for the transition from amphibolite through garnet amphibolite and hornblende eclogite to eclogite, using tholeiitic basalt as starting materials (for details, see LIU et al., 1996). These P-T transition zones are defined by (1) garnet-in, (2) plagioclase-out, and (3) amphibole-out lines. The P-T position for the solidus of tholeiite + 4 wt% H<sub>2</sub>O from these experiments and the coesite-quartz transition determined by BOHLEN and BOETTCHER (1982) are also shown.

Titanite, ilmenite, and rutile are titanium-rich phases coexisting with the silicates and/or melt. Synthesis fields for the Ti-phases are delineated in figure 2: rutile is present – and presumably stable – at high pressures ( $P > 1.6$  GPa at  $T \geq 800$  °C,  $P > 1.4$  GPa at 700 °C), ilmenite at low pressures and high temperatures ( $P < 1.6$  GPa at  $T \geq 800$  °C), and titanite at low pressures and low temperatures ( $P < 1.4$  GPa at 700 °C). Inasmuch as these Ti-rich phases are not related to one another by simple polymorphic transitions, two or even three of them may coexist under certain physicochemical conditions; but these details were not investigated experimentally. Clearly the Fe/Mg ratio of the host rock will influence the stability field of ilmenite, and the normative Ab/An ratio will affect the presence or absence of titanite. None-the-less,

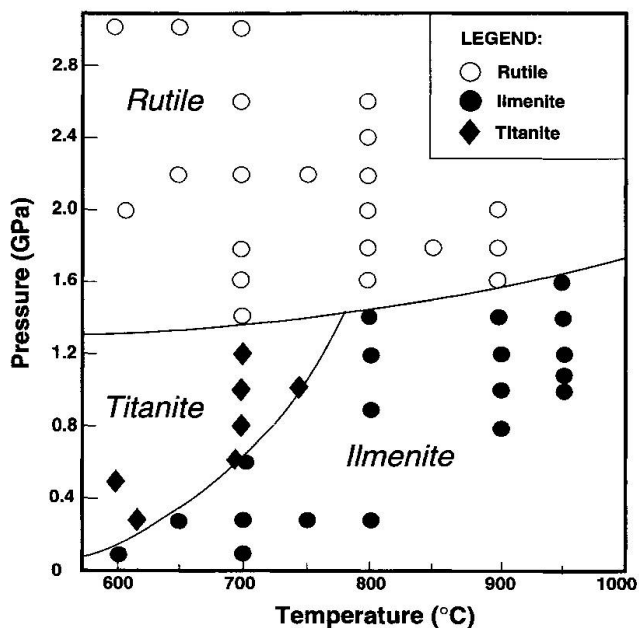


Fig. 2 Experimentally determined relations of rutile, titanite, and ilmenite for a tholeiitic basalt composition. These phases were identified in the run products and the P-T field boundaries were not reversed, hence should be considered as synthesis boundaries.

the experimentally determined growth fields illustrated in figure 2 are topologically consistent with natural occurrence of Ti-phases, lending credence to the interpretation that laboratory results closely approximate stability relations. Rutile, ilmenite, and titanite are common in eclogites, granulites + high-rank amphibolites, and greenschists + low-rank amphibolites, respectively.

### Regional geologic setting of the Gruppo di Voltri eclogites

The Gruppo di Voltri Complex of Western Liguria contains the largest ultramafic mass exposed in the Central and Western Alps. Lenses and layers of eclogitic rocks up to 4 km long and more than 200 m thick are distributed within the Beigua serpentinite. Extensive geologic and petrologic/tectonic studies of these eclogitic rocks have been carried out by MOTTANA and BOCCHIO (1975); CORTESOGNO et al. (1977); ERNST (1976, 1981); MESSIGA et al. (1983); MESSIGA and SCAMBELLURI (1988, 1991); FORCE (1991); SCAMBELLURI et al. (1991); VISSERS et al. (1991); HOOGERDIJN et al. (1993), and VALLIS and SCAMBELLURI (1996). One of these bodies, Piampaludo (shown in Fig. 3), was selected for detailed investigation in order to determine the paragenesis of Ti-bearing phases during high-P and subsequent retrograde metamorphism.

As shown in figure 3A, three distinct lithologic groups occur in the Western Ligurian Alps: (1) fully serpentinized Beigua ultramafic units containing layers of metagabbroic rocks, now converted to eclogitic, glaucophanic, barroisitic and prasinitic (greenschistic) mineral assemblages (parental rocks were both leucogabbros and ferrogabbros); (2) a diverse suite of metamorphosed volcanogenic sedimentary rocks, including the "calcescisti" (= *schistes lustrés* of the Western Alps), metamorphic rocks of the Sestri-Vtaggio zone, and sialic basement such as the Savona granite; and (3) the Erro-Tobbio lherzolites, possessing a tectonic fabric, both fresh and more-or-less serpentinized equivalents. The first and third groups of rock comprise the largely ultramafic Voltri Massif, whereas the second includes meta-igneous and metasedimentary units belonging to the Gruppo di Voltri, and other lithologic units, the initial formations of which were unrelated to the mafic/ultramafic Voltri Massif. Units (1) and (2) are interpreted as belonging to oceanic and suboceanic portions of the European-Tethyan plate, whereas unit (3) represents a mantle segment of the South Alpine realm (ERNST 1976, 1981; SCAMBELLURI et al., 1991; VISSERS et al., 1991; HOOGERDIJN et al., 1993).

Beigua ultramafic rocks are strongly sheared, antigoritic serpentinites and serpentine schists; primary mantle phases of the pre-existing peridotite have not been found. Lenses of interlayered mafic units exhibit abundant textural and mineralogic relics however, proving that the original gabbros passed through a complex series of recrystallization events, beginning with near-surface rodingitization accompanying serpentinization of the host peridotite rocks, the production of eclogitic assemblages, followed successively by glaucophanic and barroisitic stages, and terminating with the formation of greenschistic assemblages. These mafic metamorphic rocks occur as layers completely surrounded by serpentinite; probably the initial geologic setting of the precursor gabbroic bodies was chiefly as dikes and sills in suboceanic mantle peridotite.

The investigated eclogitic Fe+Ti-rich metagabbro crops out near Piampaludo, NW Italy. This body is entirely immersed in serpentinite and its contacts are irregular. Along its margins, some of the rocks have been metasomatized to rodingitic compositions; these lithologies are depleted in  $\text{SiO}_2$ , and are higher in  $\text{Al}_2\text{O}_3$  and  $\text{CaO}$ , but exhibit slightly lower  $\text{TiO}_2$  contents compared with metagabbroic rocks near the center of this body. In exploring for Ti ore deposits, numerous bore holes have been drilled and core samples collected. Sample localities of the studied metagabbroic

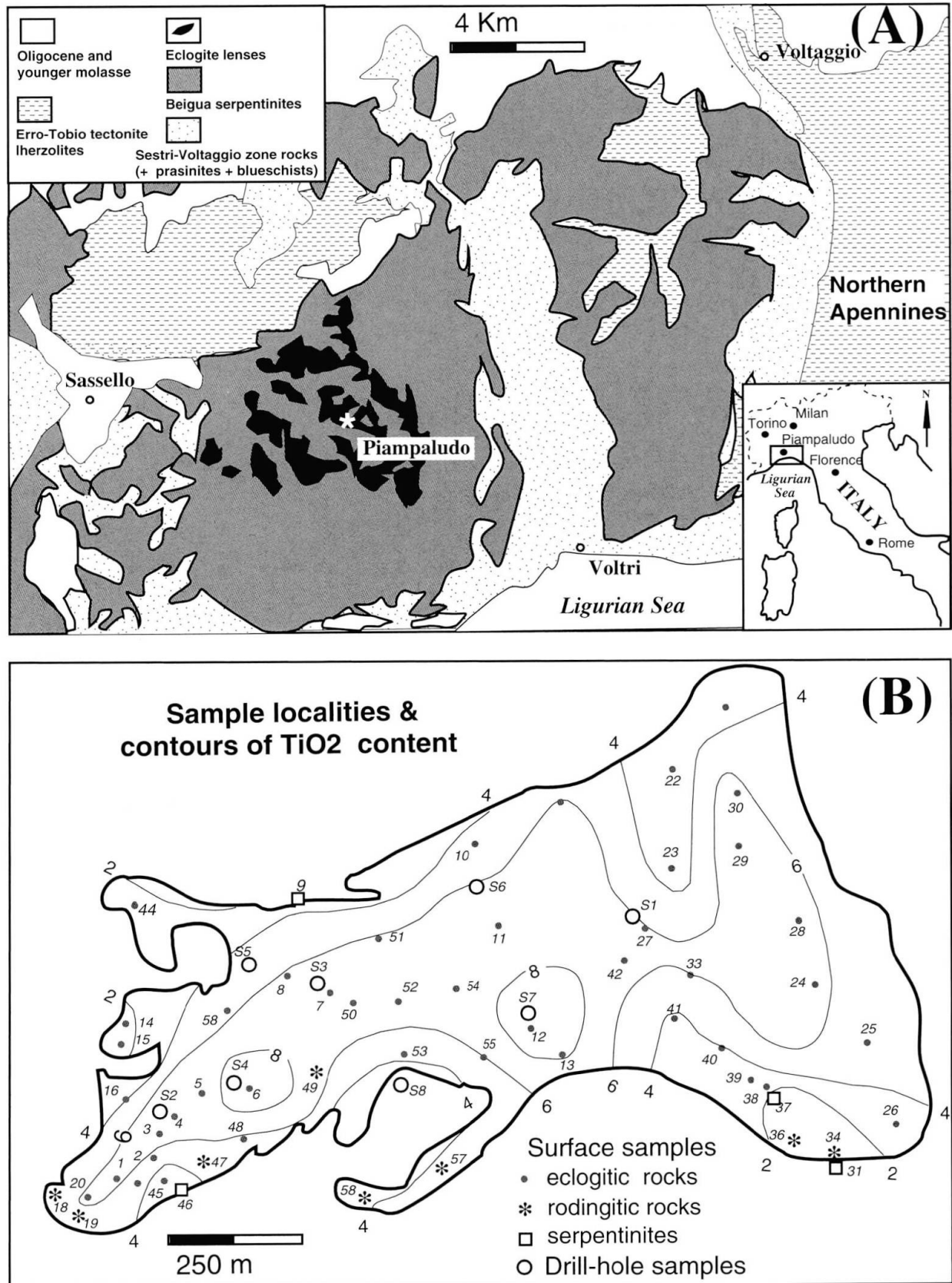


*Fig. 3* Index map of Liguria, northwestern Italy, regional geology of the Gruppo di Voltri and localities for the studied samples of eclogitic, metarodingitic and serpentinite rocks from the Piampaludo Fe+Ti-rich metagabbro body. Map units shown in (A) are modified after CORTESOGNO et al. (1977). Contours of TiO<sub>2</sub> contents at 2, 4, 6 and 8 wt% for investigated metagabbroic rocks of the Piampaludo body are shown in (B). Sample numbers are indicated by italics; those with S prefixes are drill-hole numbers.

body are shown in figure 3B. Solid circles using PR as prefix for the sample number denote surface samples, whereas open circles represent vertical drill sites (e. g., S2, S3, S4, S5 and S6). The number after the drill site refers to the depth in meters. Drill sites S1, S7, S8 and S9 are shown in figure 3B, but while they provide petrologic control for the body, core samples were unavailable for our study of these localities.

### Bulk-rock chemistry of the Gruppo di Voltri eclogites

The major-element chemistry of most of the investigated Fe+Ti-rich eclogitic samples was analyzed employing conventional XRF methods; representative analyses are listed in table 1 and graphically shown in a conventional AFM diagram as figure 4. Combined with petrographic data described below, it is clear that most of the eclogitic rocks are remarkably titanium- and iron-rich compared to common terrestrial basaltic rocks, and represent the crystallization products of an evolved melt along a tholeiitic trend (MOTTANA and BOCCHIO, 1975). Analyzed serpentinites are high in MgO, and low in both alkalis and total Fe. Piampaludo eclogitic samples are rather homogeneous in terms of major-element chemistry.  $K_2O$  contents range between 0.01–0.19 wt%,  $TiO_2$  from 1.2–9.1 wt% (most are over 5.0 wt%), total Fe as  $Fe_2O_3$  from 13.0–22.0 wt% (most exceed 18 wt%) and  $SiO_2$  from 43–49 wt%. These chemical

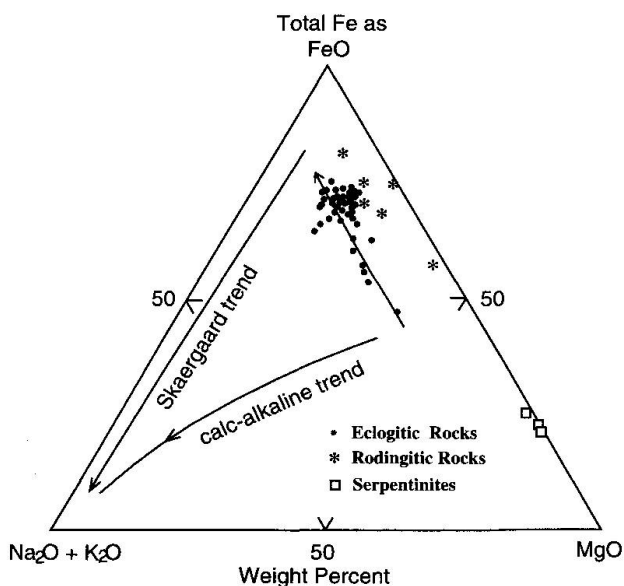


Fig. 4 Conventional AFM diagram for XRF analyses of eclogitic and meta-rodingitic rocks and serpentinites from the Piampaludo body. Compositions of Fe+Ti-rich eclogitic rocks lie along the Skaergaard tholeiitic trend.

characteristics compare favorably with ferrogabbroic oceanic tholeiites. CORTESOGNO et al. (1977) suggested that the parental gabbros were too iron- and Ti-rich to have been generated *in situ* from the enclosing Beigua ultramafic body. Instead, they may represent crystallization products of mafic magma derived elsewhere and injected at an already advanced stage of differentiation as a series of layers into relatively depleted mantle material. The gabbroic rocks were partially rodingitized during low-pressure serpentinization of the enclosing ultramafics. As shown in table 1, metarodingitic rocks exhibit much broader chemical compositions; some are remarkably enriched in CaO and depleted in alkalis and others are high in MgO and FeO, suggesting subsequent Mg-metasomatism. These mafic and ultramafic units were then subjected to eclogite-facies and retrograde metamorphism, as demonstrated by the fact that all chemical varieties of the gabbroic rocks, including the rodingites, display high-pressure mineral parageneses and later back-reaction products.

Contours of bulk-rock  $TiO_2$  contents for the analyzed samples are also shown in figure 3B. A few eclogitic rocks in the core contain more than 8 wt%  $TiO_2$ , whereas some metarodingitic rocks have less than 2 wt%  $TiO_2$ . It appears that high-Ti eclogites are mainly confined to the interior of the body, whereas samples from the margins at the contact with serpentinite tend to contain lower  $TiO_2$  contents and display the effects of advanced retrogression. Such features are quite irregular, and suggest the possible loss of Ti during either rodingitization of the gabbroic body or retrogression of the eclogitic rocks. However, available data do not allow quantification of the effect nor discrimination between these processes. Further investigation is required to solve this intriguing problem.

### Petrography of the rutile-bearing eclogites

More than 100 rutile-bearing eclogites and retrograded amphibolite/blueschist- and greenschist-facies rocks from Piampaludo were examined. They consist of 70–80 vol. % Cpx, Grt, and various types of Amp (glaucofane, barrosite, actinolite) in addition to minor Phn, Ap, Ep, Tlc, Qtz, Ab, pyrite, and Chl. Ubiquitous Ti-phases include rutile, ilmenite, and titanite. Based on megascopic structures, the Fe+Ti-rich eclogitic rocks are divided into massive varieties in the core of the body, and foliated, retrograded rocks along faults and block margins. Major petrographic features are described below:

Tab. 1 XRF analyses of representative eclogites, metarodngites and serpentinites from the Piampaludo body, Gruppo di Voltri, Italy.

|                                | Eclogitic rocks |       |       |        |        |         |       |              |       |       |        |        |  |
|--------------------------------|-----------------|-------|-------|--------|--------|---------|-------|--------------|-------|-------|--------|--------|--|
|                                | Pr-38           | Pr-39 | Pr-45 | Pr-48  | Pr-54  | Pr-55   | Pr-56 | Pr-57        | S3-28 | S3-36 | S3-82  | S3-103 |  |
| SiO <sub>2</sub>               | 46.26           | 44.58 | 45.51 | 44.87  | 45.29  | 45.18   | 46.07 | 47.88        | 43.66 | 44.02 | 46.49  | 49.38  |  |
| TiO <sub>2</sub>               | 4.71            | 6.33  | 5.52  | 5.46   | 5.97   | 5.59    | 4.21  | 4.00         | 6.28  | 6.18  | 4.34   | 2.14   |  |
| Al <sub>2</sub> O <sub>3</sub> | 11.20           | 11.17 | 11.04 | 12.23  | 11.92  | 12.33   | 11.13 | 12.32        | 11.57 | 11.92 | 12.57  | 14.68  |  |
| Fe <sub>2</sub> O <sub>3</sub> | 18.31           | 20.54 | 18.25 | 19.00  | 19.15  | 19.63   | 17.33 | 17.35        | 19.69 | 19.95 | 20.92  | 12.36  |  |
| MnO <sub>2</sub>               | 0.26            | 0.32  | 0.35  | 0.29   | 0.30   | 0.32    | 0.24  | 0.27         | 0.28  | 0.24  | 0.34   | 0.20   |  |
| MgO                            | 5.50            | 5.30  | 5.00  | 5.20   | 5.40   | 5.10    | 4.50  | 4.60         | 6.00  | 5.50  | 4.00   | 6.60   |  |
| CaO                            | 9.63            | 8.01  | 8.80  | 7.33   | 8.05   | 7.93    | 10.11 | 6.92         | 8.41  | 8.12  | 7.57   | 10.35  |  |
| K <sub>2</sub> O               | 0.00            | 0.02  | 0.04  | 0.14   | 0.00   | 0.00    | 0.04  | 0.19         | 0.03  | 0.05  | 0.00   | 0.15   |  |
| Na <sub>2</sub> O              | 4.20            | 3.60  | 5.00  | 4.40   | 4.10   | 4.10    | 5.40  | 6.00         | 3.30  | 3.40  | 4.50   | 3.60   |  |
| V <sub>2</sub> O <sub>5</sub>  | 0.09            | 0.15  | 0.07  | 0.08   | 0.11   | 0.07    | 0.06  | 0.05         | 0.19  | 0.17  | 0.03   | 0.06   |  |
| Sum                            | 100.11          | 99.98 | 99.54 | 99.08  | 100.26 | 100.23  | 99.01 | 99.50        | 99.45 | 99.53 | 100.69 | 99.49  |  |
|                                | Metarodngite    |       |       |        |        |         |       | Serpentinite |       |       |        |        |  |
|                                | Pr-35           | Pr-42 | Pr-47 | Pr-49  | S4-85  | S6-45.3 | S6-50 | Pr-37        | Pr-46 |       |        |        |  |
| SiO <sub>2</sub>               | 35.95           | 43.26 | 40.92 | 42.71  | 42.60  | 36.21   | 42.90 | 38.78        | 41.38 |       |        |        |  |
| TiO <sub>2</sub>               | 3.51            | 7.03  | 5.50  | 7.10   | 3.50   | 7.11    | 6.71  | 0.13         | 0.11  |       |        |        |  |
| Al <sub>2</sub> O <sub>3</sub> | 13.63           | 10.79 | 11.16 | 10.88  | 10.74  | 8.32    | 11.84 | 2.41         | 1.64  |       |        |        |  |
| Fe <sub>2</sub> O <sub>3</sub> | 14.87           | 21.31 | 18.56 | 21.68  | 23.93  | 19.85   | 17.08 | 9.01         | 9.00  |       |        |        |  |
| MnO <sub>2</sub>               | 0.28            | 0.28  | 0.30  | 0.29   | 0.34   | 0.43    | 0.24  | 0.14         | 0.12  |       |        |        |  |
| MgO                            | 5.40            | 6.00  | 5.90  | 6.30   | 6.70   | 15.60   | 6.40  | 37.30        | 36.00 |       |        |        |  |
| CaO                            | 24.15           | 8.69  | 9.91  | 8.22   | 7.09   | 8.31    | 10.01 | 0.01         | 0.05  |       |        |        |  |
| K <sub>2</sub> O               | 0.01            | 0.02  | 0.10  | 0.04   | 0.20   | 0.01    | 0.05  | 0.00         | 0.01  |       |        |        |  |
| Na <sub>2</sub> O              | 0.30            | 2.60  | 3.50  | 2.90   | 2.10   | 1.10    | 3.40  | 0.20         | 0.10  |       |        |        |  |
| V <sub>2</sub> O <sub>5</sub>  | 0.06            | 0.13  | 0.17  | 0.20   | 0.02   | 0.15    | 0.16  | 0.00         | 0.00  |       |        |        |  |
| Sum                            | 98.18           | 99.15 | 96.04 | 100.29 | 97.25  | 97.01   | 98.76 | 87.94        | 88.35 |       |        |        |  |

### MASSIVE ECLOGITES

Massive eclogites include both equigranular and porphyroblastic types; in general, they preserve relict gabbroic textures. Parental gabbros first underwent an eclogite-facies metamorphic event involving quasi-static conditions. Omphacitic pyroxene, garnet, and rutile developed in rocks in which the original igneous plagioclase and Ti-augite were almost perfectly pseudomorphed. Porphyroblastic minerals are mainly clinopyroxenes that epitaxially replaced primary augite. This replacement, together with granular aggregates of Grt + Amp pseudomorphing plagioclase, aggregates of fine-grained Rt + Amp after primary hornblende, and rutile-rich domains replacing primary ilmenite, define the coarse-grained original gabbroic texture. Although relict ophitic texture is not apparent due to intense recrystallization, domain replacement by neoblastic phases suggests that the protolith was Fe+Ti-rich gabbro.

*Porphyroblastic eclogites:* Porphyroblasts include coarse-grained (1–3 mm in grain size) clinopyroxenes (e.g., S2-0 and S2-5) and amphiboles (e.g. S2-15, S2-25 and S4-44), set in a fine-

grained matrix of Grt (0.05–0.6 mm), Cpx, Rt and secondary Amp, Ep, Qtz, Ab, and Chl. Some Cpx porphyroblasts have been replaced by both Ca- and Na-amphiboles; coarse-grained relict amphiboles contain exsolved rutile grains along cleavages, suggesting that rutile and fine-grained amphibole formed after coarse-grained Ti-rich primary hornblende (Fig. 5A). Euhedral garnet neoblasts range from 0.05 to 0.6 mm in diameter. Both green and violet-blue secondary amphiboles occur as fibrous, prismatic, or irregular grains enclosing garnet in the matrix, and together with chlorite as interstitial crystals between garnets. In sample PR24, coarse-grained omphacite porphyroblasts contain rounded inclusions of garnet ± talc (Fig. 5B); textural relation indicates the stable coexistence of Grt + Tlc + Omp. Some talc inclusions are replaced by blue amphibole. This assemblage of Grt + Omp + Tlc suggests very high-P metamorphism of the eclogitic rocks prior to an amphibolite/blueschist-facies overprint.

*Equigranular eclogite:* Nearly equigranular eclogite (e.g., S3-42) consists of omphacite (1–3 mm), garnet (1–2.5 mm), and later amphibole (2–2.5 mm) together with ubiquitous Ti-bearing

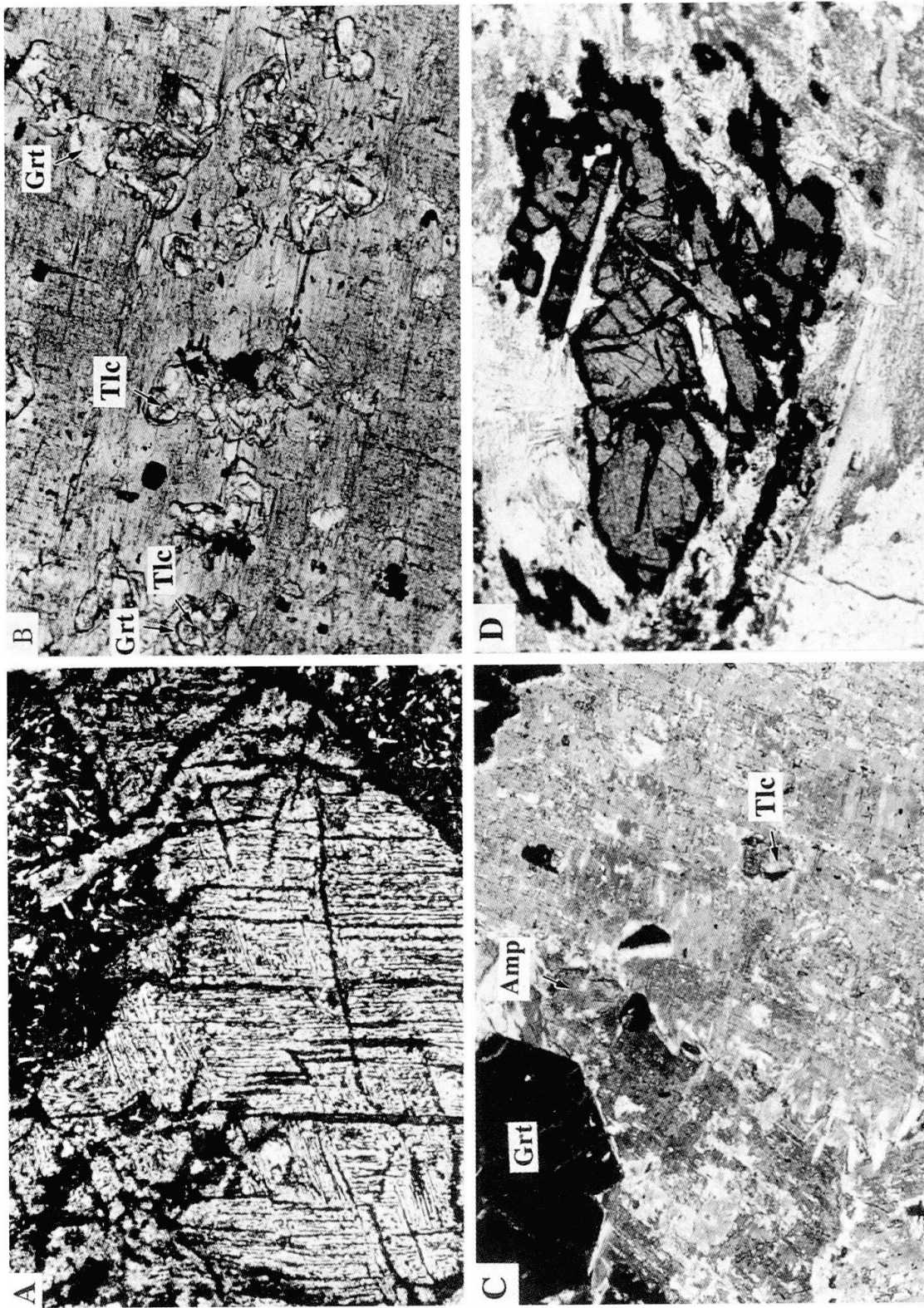


Fig. 5 Photomicrographs of few selected samples showing special parageneses of minerals from rutile-bearing eclogites from Gruppo di Voltri, Italy: (A) Exsolved rutile (rimmed by ilmenite) along cleavages of primary amphiboles (now katochlorite aggregates); such intergrowth suggests high-Ti content in primary amphibole (plane light, width of view = 1.44 mm). (B) Inclusions of garnet + talc in a porphyroblastic omphacite. Some talc crystals are rimmed by fine-grained sodic amphibole (plane light, width of view = 1.44 mm) (PR24). (C) Inclusions of talc in a porphyroblastic omphacite; retrograde Na-amphibole occurred along cleavages of Cpx (crossed polars, width of view = 1.44 mm) (PR 42). (D) Coarse-grained rutile aggregates in fine-grained amphibole; rutile grains are rimmed by ilmenite along fractures and grain margins (plane light, width of view = 1.44 mm) (PR24).

phases. Omphacite contains minor talc inclusions (Fig. 5C) and is fractured and replaced by various types of amphibole. Anhedronal garnets are fractured and filled with gradationally zoned amphiboles exhibiting light-blue Na-amphibole cores and deep-green Na-Ca amphibole rims. Pale yellow, coarse-grained amphiboles show a similar complex zoning, and were formed at the expense of omphacite and garnet. Chlorite and minor epidote are the last phases to have crystallized. Irregular aggregates of fibrous blue-green Na-amphiboles occur in the matrix and replace coarse-grained amphibole and omphacite. Silicate mineral textures in this sample suggest that Grt + Omp + Rt were the product of eclogite-facies metamorphism. Zoned Na-rich to Na-Ca amphiboles + Chl + Ep + Ab constitute the retrograde assemblage. Albite, chlorite, amphibole, and ilmenite occur in cracks of subrounded, cataclastic garnet. Rutile constitutes about 4 vol. % and occurs as irregular patches (Fig. 5D); some grains are retrograded to ilmenite along their margins.

#### FOLIATED ECLOGITES

Foliated amphibole-rich eclogites occur at the margins of the mafic bodies (e.g., Pr14 and Pr10) and at a depth of 116 meters in drill hole (S2-116). Its occurrence at such depth suggests that this mass is at least 120 meters thick. The foliation is defined by the alignment of elongate ilmenite and amphibole grains; deformation may have been concurrent with retrograde metamorphism. Based on the abundance of the Ti-bearing phase, foliated eclogites are divided into ilmenite-rich and rutile-rich types.

*Ilmenite-rich eclogitic rocks:* Such lithologies (S2-116 and PR8) contain clinopyroxene (0.5–2.5 mm) and nearly equigranular garnet set in a matrix of retrograde blue-green, fine-grained prismatic to fibrous amphiboles. Minor Qtz + Ab + Chl are present in sample S2-116. The clinopyroxene is gray-brown due to very fine exsolved minerals, and is partly replaced by amphibole. In S2-116, the Ti-bearing phase is mainly ilmenite, which occurs as isolated grains and irregular masses; minor relict rutile is rimmed by patches of ilmenite and titanite. Sample PR8 exhibits a similar texture, but a slightly different assemblage: ilmenite is the main Ti-bearing phase and occurs as isolated grains or irregular masses ranging from 0.5–2.5 mm in length.

*Rutile-bearing glaucophane eclogite:* Glaucophane-bearing eclogites (PR11 and PR21) are composed of prismatic omphacite, fine-grained garnet (0.02–0.05 mm), and interstitial glaucophane,

apatite, and quartz. Omphacite has been replaced by blue amphibole along grain margins. Rutile patches are elongated and parallel to the foliation.

#### Parageneses and compositions of silicate minerals

Petrographic observation of eclogitic and glaucophanitic samples from the Piampaludo body suggests that Rt-bearing eclogites had a complex, multistage crystallization history. At least three main stages are recognized: (1) a primary magmatic, pre-eclogite stage followed by crustal-level incipient alteration (rodingitization); (2) an eclogite-facies metamorphic stage; and (3) several retrograde metamorphic stages (glaucophanitic, barroisitic, and actinolitic amphibole overprintings). The mineral parageneses are shown in figure 6.

The first stage is identified by the occurrence of relict gabbroic textures, particularly in the massive eclogites; protoliths may retain Ti-augite, Pl, Ilm (+ Mag) and Ti-rich hornblende. These phases are pseudomorphed by aggregates of secondary phases. For example, magmatic Ti-Fe oxide domains are altered to magnetite, rutile, and minor amphibole; igneous Ti-rich hornblendes are transformed to katophorites with rutile exsolution lamellae aligned along amphibole cleavages (Figs 5A, 7A); primary augites are modified to omphacitic clinopyroxenes; and plagioclase laths are replaced by Grt + Omp ± Ep.

Parageneses of minerals from Piampaludo rutile-bearing eclogites

|                | Magmatic Stage* | Metamorphic Stage |                   |
|----------------|-----------------|-------------------|-------------------|
|                |                 | Eclogite Facies   | Blueschist Facies |
| Garnet         | _____           | _____             | _____             |
| Augite         | _____           | _____             | _____             |
| Omphacite      | _____           | _____             | _____             |
| Chloromelanite | _____           | _____             | _____             |
| Aegirine-Aug   | _____           | _____             | _____             |
| Ti-hornblende  | _____           | _____             | _____             |
| Katophorite    | _____           | _____             | _____             |
| Glaucophane    | _____           | _____             | _____             |
| Plagioclase    | _____           | _____             | _____             |
| Albite         | _____           | _____             | _____             |
| Epidote        | _____           | _____             | _____             |
| Quartz         | _____           | _____             | _____             |
| Chlorite       | _____           | _____             | _____             |
| Talc           | _____           | _____             | _____             |
| Magnetite      | _____           | _____             | _____             |
| Ilmenite       | _____           | _____             | _____             |
| Rutile         | _____           | _____             | _____             |
| Titanite       | _____           | _____             | _____             |

\*Suggested primary phases based on preserved relict textures.

Fig. 6 Parageneses of minerals from Piampaludo rutile-bearing eclogites.

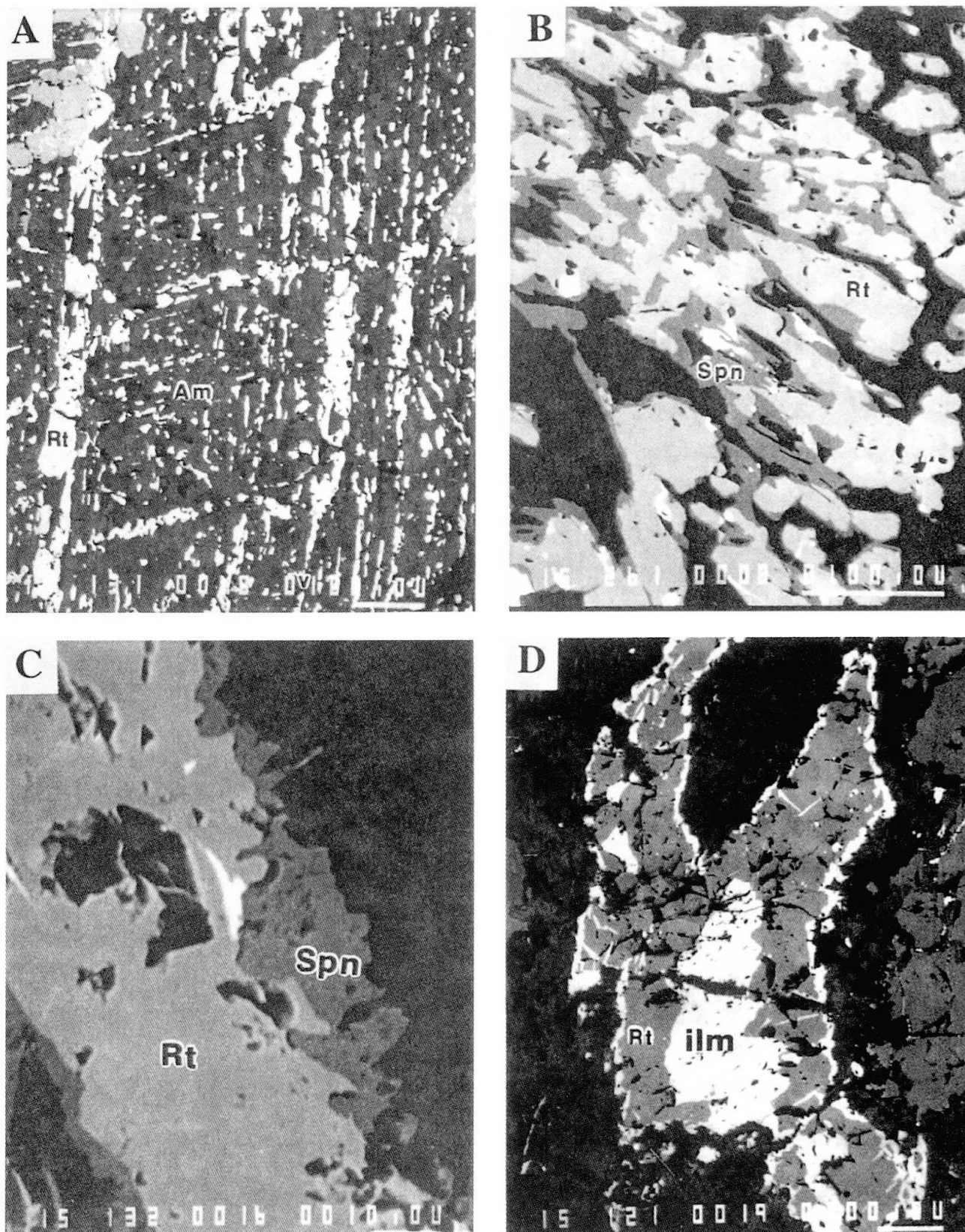


*Fig. 7* Backscattering images of Fe-Ti oxides from Piampaludo rutile-bearing eclogites (scale bar is shown in each separate photo): (A) Rutile lamellae (+ ilmenite) exsolved from coarse-grained amphibole along [110] cleavages (S2-15). (B) Paragenetic sequence of rutile - ilmenite - titanite from core to rim in sample S4-42. (C) Titanite rims around rutile grains in rutile patch. Some rutile grains are mantled successively by ilmenite and titanite (S2-25). (D) Ilmenite + rutile patch showing (1) ilmenite rimming rutile at the margins and along cracks at the center; and (2) fine-grained ilmenite needles exsolved from rutile (Pr45).

The second stage is defined by the coexistence of omphacitic pyroxene + Grt + Rt + Tlc  $\pm$  Na-amphibole. Garnets were produced through the interaction of parental igneous augite with plagioclase. Although the former usually is transformed into a single omphacitic pyroxene pseudomorph, the latter generally is replaced by a fine-grained aggregate of diversely oriented chloromelanitic crystals. Rutile derived from igneous ilmenite, as inferred from preserved skeletal structures, is present as clusters of small prismatic grains, and in some occurrences partially encompasses relict clinopyroxene.

The retrograde stages are identified by assemblages of earlier chloromelanite or aegirine-augite, sodic amphibole  $\pm$  barroisite, and later Act, Chl, Ep, Qtz, and Ab. Coarse-grained sodic amphibole grew at the expense of chloromelanite, and partly also replaced garnet. Complex intergrowths indicate the possible synchronous crystallization of glaucophane + chloromelanite. Eclogitic rutile is rimmed by ilmenite (Figs 5D, 7B), which in turn, is surrounded by titanite (Fig. 7C). Fractures transacting garnets are filled by titanite, albite, chlorite, and actinolite; these greenschist-facies minerals formed as the latest assemblages in both massive and foliated eclogitic samples.

Chemical analyses of selected minerals from representative samples were obtained by electron microprobe at Stanford University and at the University of California, Davis. The operating conditions were 15 kv accelerating potential at a beam current of 12 nA (Stanford) or 10 nA (UC Davis).

#### GARNET

Compositions of garnets from several eclogitic samples were analyzed; results are listed in table 2 and plotted in figure 8A. All iron was assumed to be divalent; this assumption appears to be realistic judging from the fact that cation totals closely approach 8.00. The analyzed garnets are poor in pyrope, and very rich in almandine, reflecting the Fe+Ti-rich nature of the bulk rock. Except for a few garnets, most analyses contain appreciable MnO (1–4 wt%), and exhibit the compositional range Alm<sub>65–85</sub>Sps<sub>0.3–4.0</sub>Grs<sub>8–28</sub>Prp<sub>3–10</sub>. However, garnets tend to be homogeneous within an individual specimen.

#### CLINOPYROXENE

Compositions of analyzed Cpx are listed in table 3. Cation proportions were estimated by normal-

izing to six oxygens; jadeite, acmite and augite end-members were calculated and plotted in the Jd-Acm-Augite diagram (Fig. 8B). Clinopyroxenes lie mainly in the compositional fields of omphacite and chloromelanite; a few plot in the aegirine-augite field. Margins of some grains are augite in sample S2-116, and the Jd and Acm components range from 13–40 and 20–30 mol%, respectively. Most pyroxenes are heterogeneous, even in a single grain, and have been partially replaced by amphibole. Clinopyroxenes from rutile-rich rocks contain higher jadeite contents than those from metarodingitized lithologies.

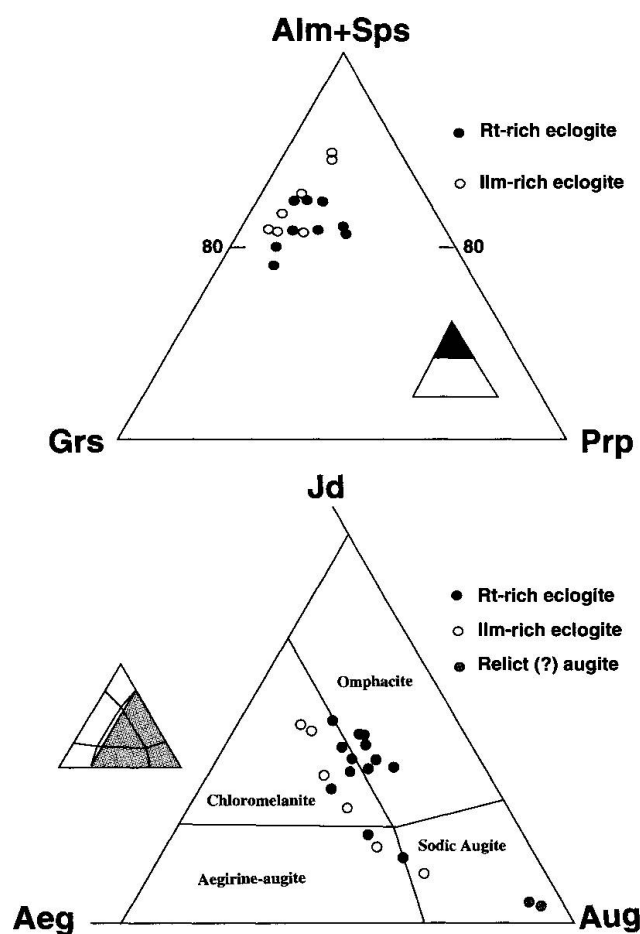


Fig. 8 Compositions of analyzed garnet and clinopyroxene from rutile-rich and ilmenite-rich eclogites, Gruppo di Voltri.

#### AMPHIBOLE

Clinoamphiboles show strong variation in composition, from sodic through calcic-sodic to calcic amphibole (Tab. 4). Paragenetic and compositional changes of this phase were presented by ERNST (1976) and ERNST and LIU (in press). Some barroisite and Na-actinolite formed as porphyro-

Tab. 2 Microprobe analyses of representative garnets from Rt-bearing eclogite from Gruppo di Voltri, Italy.

| Sample                         | PR8   | PR8   | PR24   | PR24   | PR24   | PR38   | PR38   | PR39   | S2-15 | S2-15  | S2-116 | S3-42  | S3-42  |
|--------------------------------|-------|-------|--------|--------|--------|--------|--------|--------|-------|--------|--------|--------|--------|
| texture                        |       |       |        | c      | r      | c      | r      |        |       |        |        |        |        |
| SiO <sub>2</sub>               | 36.27 | 36.03 | 37.95  | 38.07  | 37.68  | 38.11  | 37.67  | 38.00  | 37.47 | 38.29  | 36.95  | 37.45  | 37.45  |
| TiO <sub>2</sub>               | 0.06  | 0.00  | 0.02   | 0.17   | 0.20   | 0.09   | 0.27   | 0.13   | 0.14  | 0.10   | 0.10   | 0.04   | 0.04   |
| Cr <sub>2</sub> O <sub>3</sub> | 0.00  | 0.02  | 0.05   | 0.00   | 0.00   | 0.05   | 0.00   | 0.07   | 0.05  | 0.01   | 0.01   | 0.09   | 0.09   |
| Al <sub>2</sub> O <sub>3</sub> | 20.20 | 20.26 | 20.89  | 21.40  | 21.89  | 20.81  | 21.36  | 20.93  | 20.70 | 21.31  | 20.46  | 20.98  | 20.98  |
| FeO                            | 33.26 | 37.92 | 30.11  | 31.24  | 34.11  | 29.49  | 33.11  | 33.26  | 30.83 | 34.79  | 32.07  | 35.98  | 35.98  |
| MnO                            | 1.60  | 1.14  | 1.69   | 0.61   | 0.45   | 1.96   | 0.60   | 0.86   | 1.85  | 0.17   | 2.25   | 1.07   | 1.07   |
| MgO                            | 0.76  | 1.26  | 0.69   | 1.22   | 1.63   | 0.97   | 1.31   | 1.16   | 1.28  | 2.42   | 1.26   | 1.37   | 1.37   |
| CaO                            | 5.97  | 2.75  | 9.83   | 8.52   | 4.97   | 9.78   | 5.65   | 8.10   | 7.25  | 4.03   | 6.37   | 4.91   | 4.91   |
| Na <sub>2</sub> O              | n.d   | n.d   | n.d    | 0.06   | 0.02   | 0.00   | 0.04   | n.d    | n.d   | n.d    | n.d    | n.d    | n.d    |
| Total                          | 98.12 | 99.38 | 101.23 | 101.22 | 100.93 | 101.26 | 100.01 | 100.51 | 99.54 | 101.11 | 99.45  | 101.89 | 101.89 |
| Si                             | 3.007 | 2.978 | 3.020  | 3.011  | 2.995  | 3.027  | 3.021  | 2.998  | 3.029 | 3.032  | 3.012  | 2.991  | 2.991  |
| Ti                             | 0.004 | 0.000 | 0.001  | 0.010  | 0.012  | 0.005  | 0.016  | 0.008  | 0.009 | 0.006  | 0.006  | 0.002  | 0.002  |
| Cr                             | 0.000 | 0.001 | 0.003  | 0.000  | 0.000  | 0.003  | 0.000  | 0.004  | 0.003 | 0.001  | 0.000  | 0.006  | 0.006  |
| Al                             | 1.974 | 1.974 | 1.960  | 1.994  | 2.051  | 1.948  | 2.019  | 1.947  | 1.972 | 1.989  | 1.966  | 1.975  | 1.975  |
| Fe <sup>2+</sup>               | 2.306 | 2.621 | 2.004  | 2.066  | 2.268  | 1.959  | 2.221  | 2.195  | 2.084 | 2.304  | 2.186  | 2.403  | 2.403  |
| Mn                             | 0.088 | 0.062 | 0.089  | 0.032  | 0.024  | 0.103  | 0.032  | 0.045  | 0.099 | 0.009  | 0.121  | 0.056  | 0.056  |
| Mg                             | 0.094 | 0.155 | 0.082  | 0.144  | 0.193  | 0.115  | 0.157  | 0.136  | 0.154 | 0.286  | 0.153  | 0.163  | 0.163  |
| Ca                             | 0.530 | 0.244 | 0.838  | 0.722  | 0.423  | 0.832  | 0.485  | 0.685  | 0.628 | 0.342  | 0.556  | 0.420  | 0.420  |
| Na                             |       |       |        | 0.008  | 0.003  | 0.000  | 0.006  | 0.000  |       |        |        |        |        |
| Sum                            | 8.002 | 8.035 | 7.997  | 7.987  | 7.969  | 7.992  | 7.957  | 8.018  | 7.976 | 7.968  | 8.000  | 8.017  | 8.017  |
| Alm                            | 0.764 | 0.850 | 0.665  | 0.697  | 0.780  | 0.651  | 0.767  | 0.717  | 0.703 | 0.784  | 0.725  | 0.790  | 0.790  |
| Spe                            | 0.029 | 0.020 | 0.029  | 0.011  | 0.008  | 0.034  | 0.011  | 0.015  | 0.033 | 0.003  | 0.040  | 0.019  | 0.019  |
| Prp                            | 0.031 | 0.050 | 0.027  | 0.049  | 0.066  | 0.038  | 0.054  | 0.045  | 0.052 | 0.097  | 0.051  | 0.054  | 0.054  |
| Grs                            | 0.176 | 0.079 | 0.278  | 0.244  | 0.146  | 0.277  | 0.168  | 0.224  | 0.212 | 0.116  | 0.184  | 0.138  | 0.138  |

c, core; r, rim.

Tab. 3 Analyses of representative clinopyroxenes from Rt-bearing eclogite from Gruppo di Voltri, Italy.

| Sample                         | S2-15 | S2-116 | S2-116 | S2-116 | S3-42  | S3-42  | Pr8   | Pr8   | Pr11  | Pr11   | Pr24   | Pr24  | Pr45  |
|--------------------------------|-------|--------|--------|--------|--------|--------|-------|-------|-------|--------|--------|-------|-------|
| SiO <sub>2</sub>               | 55.15 | 52.85  | 53.83  | 52.14  | 56.35  | 55.84  | 55.21 | 53.95 | 55.10 | 55.23  | 55.24  | 53.04 | 52.64 |
| TiO <sub>2</sub>               | 0.06  | 0.07   | 0.00   | 0.63   | 0.09   | 0.11   | 0.26  | 0.16  | 0.02  | 0.02   | 0.04   | 0.07  | 0.31  |
| Al <sub>2</sub> O <sub>3</sub> | 6.94  | 4.78   | 2.56   | 2.36   | 9.22   | 8.00   | 8.47  | 6.60  | 7.89  | 7.48   | 6.57   | 5.26  | 4.56  |
| FeO                            | 10.05 | 12.51  | 8.04   | 10.91  | 9.09   | 10.67  | 13.74 | 13.69 | 11.10 | 11.52  | 13.09  | 12.05 | 13.84 |
| MnO                            | 0.01  | 0.03   | 0.04   | 0.28   | 0.00   | 0.01   | 0.05  | 0.02  | 0.03  | 0      | 0.06   | 0.05  | 0.20  |
| MgO                            | 7.01  | 7.34   | 11.49  | 12.59  | 6.96   | 6.81   | 4.62  | 5.61  | 6.29  | 6.78   | 6.48   | 8.02  | 6.74  |
| CaO                            | 12.15 | 13.43  | 17.84  | 20.28  | 11.40  | 11.97  | 8.49  | 11.40 | 11.74 | 12.78  | 12.03  | 14.07 | 13.39 |
| Na <sub>2</sub> O              | 7.42  | 6.21   | 4.32   | 1.24   | 7.92   | 7.42   | 8.99  | 7.65  | 7.45  | 6.87   | 7.68   | 5.69  | 6.23  |
| Total                          | 98.79 | 97.22  | 98.12  | 100.43 | 101.03 | 100.82 | 99.83 | 99.06 | 99.60 | 100.68 | 101.19 | 98.23 | 97.91 |
| Si                             | 2.046 | 2.031  | 2.027  | 1.950  | 2.024  | 2.029  | 2.045 | 2.033 | 2.033 | 2.023  | 2.032  | 2.012 | 2.025 |
| Ti                             | 0.002 | 0.002  | 0.000  | 0.018  | 0.002  | 0.003  | 0.007 | 0.004 | 0.001 | 0.001  | 0.001  | 0.002 | 0.009 |
| Al                             | 0.303 | 0.217  | 0.114  | 0.104  | 0.390  | 0.343  | 0.370 | 0.293 | 0.343 | 0.323  | 0.285  | 0.235 | 0.207 |
| Fe <sup>2+</sup>               | 0.312 | 0.402  | 0.253  | 0.341  | 0.273  | 0.324  | 0.426 | 0.431 | 0.342 | 0.353  | 0.403  | 0.382 | 0.445 |
| Mn                             | 0.000 | 0.001  | 0.001  | 0.007  | 0.000  | 0.000  | 0.001 | 0.000 | 0.001 | 0.000  | 0.001  | 0.001 | 0.005 |
| Mg                             | 0.388 | 0.421  | 0.645  | 0.702  | 0.373  | 0.369  | 0.255 | 0.315 | 0.346 | 0.370  | 0.355  | 0.454 | 0.387 |
| Ca                             | 0.483 | 0.553  | 0.720  | 0.813  | 0.439  | 0.466  | 0.337 | 0.460 | 0.464 | 0.502  | 0.474  | 0.572 | 0.552 |
| Na                             | 0.534 | 0.463  | 0.315  | 0.090  | 0.552  | 0.523  | 0.646 | 0.559 | 0.533 | 0.488  | 0.548  | 0.418 | 0.465 |
| Sum                            | 4.068 | 4.090  | 4.074  | 4.025  | 4.054  | 4.058  | 4.086 | 4.096 | 4.062 | 4.059  | 4.099  | 4.077 | 4.095 |

blasts in strongly retrograded and deformed eclogites near the margins of the metagabbro bodies. Zoned amphiboles from sodic blue-amphibole cores (glaucophane and ferroglaucophane) man-

ted by Ca-Na green amphibole formed progressively, replacing chloromelanite and omphacite, and occurring as interstitial phases along garnet grain boundaries.

Tab. 4 Microprobe analyses of amphiboles from Rt-bearing eclogite from Gruppo di Voltri, Italy

| Sample                         | S3-42  | S3-42  | S3-42  | Pr11   | Pr8    | Pr8    | S2-116 | S2-116 | S2-15  | S2-15  |
|--------------------------------|--------|--------|--------|--------|--------|--------|--------|--------|--------|--------|
| SiO <sub>2</sub>               | 55.16  | 54.16  | 55.85  | 55.42  | 56.43  | 54.46  | 44.79  | 46.80  | 47.07  | 54.84  |
| TiO <sub>2</sub>               | 0.13   | 0.07   | 0.13   | 0.02   | 0.02   | 0.04   | 0.37   | 0.16   | 0.27   | 0.33   |
| Cr <sub>2</sub> O <sub>3</sub> | 0.00   | 0.04   | 0.00   | 0.00   | 0.00   | 0.00   | 0.12   | 0.01   | 0.07   | 0.00   |
| Al <sub>2</sub> O <sub>3</sub> | 10.31  | 3.89   | 1.09   | 9.88   | 9.57   | 8.84   | 9.17   | 7.39   | 10.14  | 2.57   |
| Fe <sub>2</sub> O <sub>3</sub> | 2.24   | 1.70   | 1.63   | 2.73   | 2.16   | 4.17   | 2.27   | 2.01   | 1.71   | 1.84   |
| FeO                            | 12.23  | 11.52  | 10.36  | 11.79  | 15.55  | 14.24  | 18.96  | 14.90  | 15.54  | 11.14  |
| MnO                            | 0.09   | 0.08   | 0.00   | 0.00   | 0.01   | 0.03   | 0.20   | 0.31   | 0.12   | 0.11   |
| MgO                            | 9.29   | 14.55  | 17.02  | 9.02   | 7.21   | 7.73   | 8.47   | 11.33  | 9.14   | 15.05  |
| CaO                            | 2.28   | 9.37   | 10.79  | 1.24   | 0.56   | 0.84   | 9.57   | 10.22  | 7.58   | 9.12   |
| Na <sub>2</sub> O              | 6.43   | 2.58   | 1.16   | 6.65   | 6.87   | 6.84   | 4.04   | 3.09   | 4.46   | 2.04   |
| K <sub>2</sub> O               | 0.05   | 0.05   | 0.00   | 0.03   | 0.05   | 0.03   | 0.00   | 0.00   | 0.22   | 0.04   |
| Total                          | 98.19  | 98.01  | 98.03  | 96.78  | 98.43  | 97.20  | 97.96  | 96.20  | 96.30  | 97.08  |
| Si                             | 7.738  | 7.726  | 7.911  | 7.843  | 7.948  | 7.813  | 6.787  | 7.048  | 7.041  | 7.863  |
| Ti                             | 0.015  | 0.012  | 0.014  | 0.005  | 0.009  | 0.009  | 0.042  | 0.018  | 0.031  | 0.036  |
| Cr                             | 0.000  | 0.004  | 0.000  | 0.000  | 0.000  | 0.000  | 0.014  | 0.001  | 0.008  | 0.000  |
| Al                             | 1.703  | 0.653  | 0.182  | 1.648  | 1.589  | 1.496  | 1.637  | 1.312  | 1.789  | 0.434  |
| Fe <sup>+3</sup>               | 0.237  | 0.183  | 0.174  | 0.291  | 0.229  | 0.450  | 0.259  | 0.228  | 0.192  | 0.199  |
| Fe <sup>+2</sup>               | 1.434  | 1.375  | 1.228  | 1.396  | 1.832  | 1.709  | 2.401  | 1.878  | 1.944  | 1.336  |
| Mn                             | 0.011  | 0.010  | 0.000  | 0.000  | 0.001  | 0.004  | 0.026  | 0.039  | 0.015  | 0.013  |
| Mg                             | 1.940  | 3.092  | 3.593  | 1.902  | 1.513  | 1.652  | 1.912  | 2.541  | 2.037  | 3.216  |
| Ca                             | 0.343  | 1.432  | 1.638  | 0.188  | 0.085  | 0.128  | 1.553  | 1.649  | 1.214  | 1.401  |
| Na                             | 1.746  | 0.715  | 0.319  | 1.825  | 1.876  | 1.903  | 1.186  | 0.901  | 1.292  | 0.567  |
| K                              | 0.007  | 0.005  | 0.000  | 0.002  | 0.002  | 0.001  | 0.000  | 0.000  | 0.041  | 0.007  |
| SUM                            | 15.165 | 15.208 | 15.057 | 15.101 | 15.084 | 15.164 | 15.813 | 15.615 | 15.602 | 15.072 |

## TALC AND MINNESOTAITE

Talc occurs as tiny inclusions about 0.01 mm across in Cpx porphyroblasts in several eclogite samples. Compositions of these inclusions were analyzed from two samples (Tab. 5); they contain 5–6 wt% FeO and appear to be stable together with the host Cpx. Fe end-member talc (minnesotaite) was found as a minor retrograde phase together with an unknown phase + sodic Am in

veins cutting several eclogitic samples. Minnesotaite has optical properties similar to phengitic mica, hence microprobe analysis was necessary to confirm its identification. The analyzed minnesotaites contain very high total iron as FeO; this phase may be a common retrograde phase in these rocks inasmuch as the investigated protoliths are characterized by high Fe and Ti contents.

Tab. 5 Microprobe analyses of talc and minnesotaite in Rt-bearing eclogites from Gruppo di Voltri, Italy.

| Sample No.                     | Talc     |          | Minnesotaite |          |
|--------------------------------|----------|----------|--------------|----------|
|                                | Pr42     | Pr24     | Pr8          | Pr8      |
|                                | Stanford | Stanford | UCDavis      | Stanford |
| SiO <sub>2</sub>               | 56.38    | 57.83    | 51.56        | 49.01    |
| TiO <sub>2</sub>               | 0.02     | 0.01     | 0.06         | 0.03     |
| Al <sub>2</sub> O <sub>3</sub> | 4.22     | 3.20     | 0.11         | 0.19     |
| Cr <sub>2</sub> O <sub>3</sub> | 0.00     | 0.02     | 0.00         | 0.02     |
| FeO                            | 9.98     | 9.28     | 32.99        | 32.08    |
| MnO                            | 0.05     | 0.06     |              | 0.12     |
| MgO                            | 23.91    | 23.37    | 12.65        | 13.47    |
| CaO                            | 0.14     | 0.12     | 0.64         | 0.67     |
| K <sub>2</sub> O               | 0.01     | 0.00     | 0.00         | 0.20     |
| Na <sub>2</sub> O              | 0.10     | 0.05     | 0.07         | 0.03     |
| Total                          | 94.83    | 93.93    | 98.08        | 95.82    |

## OTHER PHASES

Ti-bearing minerals and several other phases described below were analyzed from the investigated eclogitic samples. Among the latter, pyrite, apatite, and minor goethite are most common. Goethite is a late retrograde mineral, whereas pyrite and apatite are common minor phases of the eclogite-facies assemblage.

## Occurrence and compositional characteristics of rutile, ilmenite, and titanite

Except for primary igneous ilmenite, rutile is consistently the first neoblastic Ti-bearing phase to have crystallized during eclogite stage of metamorphism in all investigated samples. It was sub-

Tab. 6 Microprobe analyses of rutile from Rt-bearing eclogite from Gruppo di Voltri, Italy.

| Type                           | I       | I       | I      | I       | I       | I       | I      | I       | I      | I      | I       |
|--------------------------------|---------|---------|--------|---------|---------|---------|--------|---------|--------|--------|---------|
| Color                          | Red B.  | Red B.  | Red B. | Gold Y. | Red B.  | Gold Y. | Red B. | Gold Y. | Red B. | Red B. | Gold Y. |
| Sample                         | S2-15   | S2-15   | S2-25  | S3-36   | S3-42   | PR2     | PR3    | PR7     | PR24   | PR38   | PR39    |
| SiO <sub>2</sub>               | 0.00    | 0.00    |        | 0.00    | 0.02    | 0.00    | 0.00   | 0.02    | 0.01   | 0.03   | 0.01    |
| TiO <sub>2</sub>               | 99.56   | 98.80   | 98.41  | 99.10   | 100.49  | 99.63   | 97.40  | 98.78   | 98.92  | 99.92  | 99.72   |
| Al <sub>2</sub> O <sub>3</sub> | 0.04    | 0.02    | 0.01   | 0.04    | 0.07    | 0.04    | 0.07   | 0.03    | 0.03   | 0.02   | 0.01    |
| FeO                            | 0.38    | 0.39    | 0.41   | 0.26    | 0.43    | 0.29    | 0.41   | 0.28    | 0.38   | 0.49   | 0.30    |
| MnO                            | 0.21    | 0.05    | 0.00   | 0.00    | 0.00    | 0.02    | 0.15   | 0.20    | 0.00   | 0.02   | 0.02    |
| CaO                            | 0.00    | 0.14    |        | 0.04    | 0.06    | 0.00    | 0.07   | 0.03    | 0.05   | 0.01   | 0.09    |
| Total                          | 100.18  | 99.41   | 98.91  | 99.44   | 101.07  | 99.98   | 99.09  | 99.32   | 99.72  | 100.47 | 100.15  |
| Type                           | I       | I       | I      | I       | I       | I       | II     | III     | III    | III    |         |
| Color                          | Gold Y. | Gray Y. | Red B. | Gold Y. | Gray Y. | Red B.  | Red B. | Red B.  | Red B. | Brown  |         |
| Sample                         | PR45    | PR48    | PR55   | PR2     | PR57    | S3-28   | S2-15  | PR3     | S2-15  | S4-42  |         |
| SiO <sub>2</sub>               | 0.01    | 0.01    |        | 0.04    | 0.00    | 0.00    |        | 0.01    | 0.04   |        |         |
| TiO <sub>2</sub>               | 97.22   | 98.86   | 100.18 | 99.29   | 99.90   | 98.75   | 97.99  | 97.34   | 97.68  | 98.27  |         |
| Al <sub>2</sub> O <sub>3</sub> | 0.02    | 0.06    | 0.02   | 0.02    | 0.02    | 0.01    | 0.02   | 0.06    | 0.04   | 0.05   |         |
| FeO                            | 0.62    | 0.00    | 0.37   | 0.31    | 0.62    | 0.35    | 0.56   | 0.50    | 0.53   | 0.33   |         |
| MnO                            | 0.03    | 0.49    | 0.00   | 0.00    | 0.05    | 0.01    | 0.00   | 0.00    | 0.10   | 0.00   |         |
| CaO                            | 0.00    | 0.02    |        | 0.01    |         | 0.12    |        | 0.32    | 0.24   |        |         |
| Total                          | 97.90   | 99.51   | 100.57 | 99.67   | 100.59  | 99.24   | 99.88  | 98.23   | 98.63  | 98.65  |         |

Type I, rutile in rutile and rutile + ilmenite patch (ilmenite > 10%); II, rutile exsolution in amphibole and III, rutile in Rt + Ilm + Ttn patch. Color: B: brown; Y: yellow.

sequently replaced by ilmenite and/or titanite along margins and cracks. Secondary ilmenite and titanite are coarse-grained and constitute more than 6 vol. % in strongly retrograded eclogites. In other samples, ilmenite and titanite are minor but ubiquitous. Very fine-grained (< 5 µm) titanite in many samples can be detected only by electron back-scattered imagery. As shown in figures 7C and D, thin layers of titanite with a thickness of 1–33 µm occur around host rutile or ilmenite. Tables 6, 7 and 8 list representative compositions of analyzed rutile, ilmenite, and titanite.

Rutile shows different colors in different samples; however, it is chemically homogeneous and consists of nearly pure, stoichiometric TiO<sub>2</sub>, with only very minor iron content. On the other hand, ilmenites of different modes of occurrence exhibit significant chemical variations, especially in MnO contents, probably due to differences in ilmenite parageneses as shown in table 7. Except for the low-Mn fine-grained ilmenite grains associated with rutile lamellae in amphibole and exsolved ilmenite needles in rutile, most analyzed ilmenites exhibit substantial variation in MnO content, ranging from 0.31 to 5.37 wt%, averaging 1.98 wt%. Both host minerals (Ti-hornblende and rutile) contain only minor MnO, hence the associated ilmenites are also low in MnO (< 0.8 wt%).

The exsolved ilmenite needles in some coarse-grained rutiles are not related to cracks or veins; their occurrence suggests higher Fe content of earlier formed rutile. Fe-bearing rutile may become unstable on decompression, and ilmenite needles apparently were exsolved during subsequent recrystallization. Some fine-grained, discrete ilmenite grains along the amphibole cleavages or in rutile patches may be a stable phase of eclogite-facies metamorphism as suggested by Felicity Lloyd (personal communication, 1997). Excess Fe for eclogitic silicates may have stabilized ilmenite in addition to rutile in these Fe+Ti-rich metagabbros. The stability of ilmenite under eclogite facies condition is critically dependent on bulk-rock composition and fugacities of oxygen and sulfur; for MORB composition, ilmenite was not detected in experimental run products under eclogite-facies conditions described by LIU et al. (1996).

Three different titanite-bearing assemblages were identified: A-type titanite associated with rutile (S-25; PR55) (Fig. 7B), B-type titanite associated with ilmenite (PR57), and C-type titanite associated with both rutile and ilmenite (S4-42, PR45, S2-116) (Fig. 7C). Textural evidence indicates that titanite was formed during retrograde metamorphism by the reaction of rutile and il-

Tab. 7 Microprobe analyses of ilmenite from Gruppo di Voltri eclogites, Italy

| Type                           | I     | I     | I     | I      | I     | I     | I     | I      | I     | I     | I      | I     | I     |
|--------------------------------|-------|-------|-------|--------|-------|-------|-------|--------|-------|-------|--------|-------|-------|
| Sample                         | S2-15 | S2-15 | PR2   | PR3    | PR3   | PR7   | PR39  | S3-36  | S3-28 | S3-28 | PR2    | PR45  | PR57  |
| SiO <sub>2</sub>               | 0.00  | 0.02  | 0.00  | 0.00   | 0.04  | 0.00  | 0.00  | 0.00   | 0.01  | 0.00  | 0.01   |       |       |
| TiO <sub>2</sub>               | 50.62 | 51.93 | 54.50 | 52.64  | 51.35 | 53.21 | 51.30 | 51.80  | 52.46 | 52.83 | 52.45  | 53.08 | 53.81 |
| Al <sub>2</sub> O <sub>3</sub> | 1.62  | 0.02  | 0.04  | 0.04   | 0.02  | 0.05  | 1.96  | 0.03   | 0.02  | 0.04  | 0.03   | 0.02  | 0.02  |
| FeO                            | 44.29 | 46.13 | 41.71 | 46.18  | 44.92 | 43.69 | 45.62 | 43.84  | 45.31 | 44.56 | 45.55  | 45.38 | 41.70 |
| MnO                            | 2.68  | 0.31  | 3.09  | 1.21   | 2.60  | 2.09  | 0.38  | 5.37   | 0.64  | 0.93  | 2.14   | 1.00  | 2.42  |
| MgO                            | 0.20  |       |       |        |       |       | 0.69  |        |       |       | 0.00   | 0.40  | 0.51  |
| CaO                            | 0.48  | 0.18  | 0.00  | 0.11   | 0.21  | 0.20  | 0.00  | 0.08   | 0.00  | 0.00  | 0.00   |       |       |
| Total                          | 99.89 | 98.59 | 99.34 | 100.18 | 99.14 | 99.24 | 99.95 | 101.12 | 98.44 | 98.36 | 100.17 | 99.88 | 98.46 |
| Si                             | 0.000 | 0.000 | 0.000 | 0.000  | 0.040 | 0.000 | 0.000 | 0.000  | 0.010 | 0.000 | 0.005  | 0.000 | 0.000 |
| Ti                             | 0.959 | 1.000 | 1.029 | 0.998  | 0.987 | 1.012 | 0.963 | 0.980  | 1.008 | 1.014 | 0.996  | 1.004 | 1.023 |
| Al                             | 0.048 | 0.000 | 0.001 | 0.001  | 0.000 | 0.050 | 0.058 | 0.000  | 0.000 | 0.001 | 0.000  | 0.000 | 0.000 |
| Fe                             | 0.933 | 0.987 | 0.875 | 0.974  | 0.960 | 0.924 | 0.953 | 0.922  | 0.968 | 0.951 | 0.962  | 0.955 | 0.882 |
| Mn                             | 0.057 | 0.007 | 0.066 | 0.026  | 0.056 | 0.045 | 0.008 | 0.114  | 0.014 | 0.020 | 0.046  | 0.021 | 0.052 |
| Mg                             | 0.008 | 0.000 | 0.000 | 0.000  | 0.000 | 0.000 | 0.026 | 0.000  | 0.000 | 0.000 | 0.000  | 0.015 | 0.019 |
| Ca                             | 0.013 | 0.005 | 0.000 | 0.003  | 0.006 | 0.005 | 0.000 | 0.002  | 0.000 | 0.000 | 0.000  | 0.000 | 0.000 |
| Total                          | 2.017 | 2.000 | 1.971 | 2.001  | 2.011 | 1.987 | 2.008 | 2.020  | 1.991 | 1.986 | 2.004  | 1.996 | 1.977 |

Type I, ilmenite in rutile patch and in rutile and ilmenite patch; IIa, with Rt exsolution lamellae in amphibole; IIb, needle in rutile; III, coarse grain; IV, disseminated; V, with rutile and titanite or with titanite.

Tab. 7 (continued)

| Type                           | IIa   | IIa    | IIb   | IIb   | IIb   | IIb    | III    | IV    | IV     | V     | V      | V     | V     |
|--------------------------------|-------|--------|-------|-------|-------|--------|--------|-------|--------|-------|--------|-------|-------|
| Sample                         | S2-2  | S2-2   | PR24  | PR24  | PR55  | S3-42  | S2-116 | S2-15 | PR3    | S2-15 | S2-116 | PR57  | S4-42 |
| SiO <sub>2</sub>               | 0     | 0.06   | 0.02  | 0.02  |       |        |        | 0.02  | 0.03   |       | 0.07   | 0.02  |       |
| TiO <sub>2</sub>               | 50.87 | 51.58  | 51.81 | 54.86 | 52.08 | 53.53  | 50.46  | 51.29 | 52.73  | 50.87 | 50.94  | 54.54 | 51.53 |
| Al <sub>2</sub> O <sub>3</sub> | 0.02  | 1.31   | 0.03  | 0.02  | 0.05  | 0.02   | 0.11   | 0.07  | 0.08   | 0.03  | 0.02   | 0.03  | 0.10  |
| FeO                            | 46.41 | 45.96  | 46.14 | 44.76 | 44.89 | 46.72  | 47.32  | 44.67 | 45.00  | 43.79 | 43.41  | 42.28 | 44.35 |
| MnO                            | 0.77  | 0.61   | 0.46  | 0.28  | 0.00  | 0.14   | 1.91   | 1.63  | 2.32   | 2.14  | 2.83   | 2.11  | 1.48  |
| MgO                            |       | 0.42   |       |       | 0.37  | 0.41   | 0.31   |       |        |       | 0.52   | 0.51  | 0.44  |
| CaO                            | 0.38  | 0.51   | 0.00  | 0.00  |       | 0.00   | 0.09   | 0.23  | 0.00   | 0.20  | 0.11   | 0.09  |       |
| Total                          | 98.45 | 100.45 | 98.46 | 99.94 | 97.39 | 100.82 | 100.23 | 97.91 | 100.16 | 97.03 | 97.90  | 99.58 | 97.90 |
| Si                             | 0.000 | 0.001  | 0.000 | 0.000 | 0.000 | 0.000  | 0.000  | 0.000 | 0.000  | 0.000 | 0.002  | 0.000 | 0.000 |
| Ti                             | 0.986 | 0.969  | 0.999 | 1.029 | 1.008 | 1.003  | 0.966  | 0.995 | 0.999  | 0.996 | 0.987  | 1.024 | 0.996 |
| Al                             | 0.000 | 0.039  | 0.000 | 0.000 | 0.002 | 0.000  | 0.003  | 0.002 | 0.002  | 0.000 | 0.000  | 0.000 | 0.003 |
| Fe                             | 1.000 | 0.960  | 0.989 | 0.934 | 0.967 | 0.974  | 1.007  | 0.964 | 0.948  | 0.954 | 0.936  | 0.883 | 0.954 |
| Mn                             | 0.017 | 0.013  | 0.010 | 0.006 | 0.000 | 0.003  | 0.042  | 0.036 | 0.049  | 0.047 | 0.062  | 0.045 | 0.032 |
| Mg                             | 0.000 | 0.016  | 0.000 | 0.000 | 0.014 | 0.015  | 0.012  | 0.000 | 0.000  | 0.000 | 0.020  | 0.019 | 0.017 |
| Ca                             | 0.010 | 0.014  | 0.000 | 0.000 | 0.000 | 0.000  | 0.002  | 0.006 | 0.000  | 0.006 | 0.003  | 0.002 | 0.000 |
| Total                          | 2.014 | 2.011  | 2.000 | 1.970 | 1.991 | 1.996  | 2.032  | 2.003 | 1.999  | 2.003 | 2.010  | 1.975 | 2.002 |

menite with Ca-bearing silicates such as omphacite or garnet. The low total (96 to 98 wt%) for some titanite analyses may reflect the presence of Al(OH)<sub>3</sub>; in most analyses, Al<sub>2</sub>O<sub>3</sub> ranges from 0.7 to 1.4 wt%.

#### Estimation of P-T conditions of metamorphism

Judging from textures, mineral assemblages, and chemical compositions described above, protoliths of the Rt-rich Piampaludo eclogitic rocks were titaniferous ferrogabbros containing consid-

erable amounts of FeO, TiO<sub>2</sub>, and MnO. These eclogites underwent a prolonged, multistage crystallization history. The earliest magmatic stage was followed by ocean-floor(?) metamorphism, which may have modified the initial bulk-rock compositions – especially near the margins of mafic bodies. Near-surface metasomatic exchanges between ultramafic country rock and associated gabbroic bodies probably resulted in the formation of rodingites prior to closure of the Tethyan ocean basin (ERNST, 1976). The second stage involved eclogite-facies metamorphism attending subduction of the European-Tethyan

Tab. 8 Compositions of titanite in Gruppo di Voltri eclogite, Italy.

| Sample                         | S2-25 | S2-116 | S4-42 | PR45  | PR55  | PR57  |
|--------------------------------|-------|--------|-------|-------|-------|-------|
| SiO <sub>2</sub>               | 29.61 | 29.83  | 29.97 | 29.36 | 29.37 | 29.97 |
| TiO <sub>2</sub>               | 40.89 | 37.75  | 39.30 | 38.86 | 37.94 | 40.33 |
| Al <sub>2</sub> O <sub>3</sub> | 0.87  | 1.43   | 0.73  | 1.03  | 1.32  | 0.94  |
| FeO                            | 0.27  | 0.49   | 0.56  | 0.72  | 0.57  | 0.79  |
| MnO                            | 0.03  | 0.04   | 0.04  | 0.00  | 0.07  | 0.00  |
| MgO                            | 0.03  | 0.01   | 0.00  | 0.00  | 0.00  | 0.02  |
| CaO                            | 27.29 | 28.85  | 28.43 | 26.53 | 27.06 | 27.46 |
| Total                          | 98.98 | 98.40  | 99.03 | 96.51 | 96.32 | 99.50 |
| Si                             | 0.975 | 0.992  | 0.990 | 0.992 | 0.980 | 0.990 |
| Ti                             | 1.015 | 0.944  | 0.977 | 0.987 | 0.990 | 0.980 |
| Al                             | 0.035 | 0.056  | 0.028 | 0.041 | 0.040 | 0.030 |
| Fe                             | 0.010 | 0.014  | 0.015 | 0.020 | 0.020 | 0.020 |
| Mn                             | 0.000 | 0.001  | 0.001 | 0.000 | 0.000 | 0.000 |
| Mg                             | 0.000 | 0.000  | 0.000 | 0.000 | 0.000 | 0.000 |
| Ca                             | 0.965 | 1.028  | 1.007 | 0.960 | 0.970 | 1.010 |
| Total                          | 3.000 | 3.035  | 3.018 | 3.000 | 3.000 | 3.030 |

plate. The last stage consisted of amphibolite/blueschist-, then greenschist-facies decompression metamorphism. Unfortunately, it is difficult to estimate the peak temperature for eclogite-facies metamorphism inasmuch as the rutile-bearing eclogitic rocks were extensively recrystallized during later retrogression. Few suitable mineral assemblages were found for P-T estimates; only a few  $K_D$  values describing Fe-Mg partitioning between coexisting garnet and clinopyroxene were calculated. The  $K_D$  values listed in table 9 range from 26 to 59. Based on the calibration of POWELL (1985), and RÄHEIM and GREEN (1974), these  $K_D$  values, adjusted for the  $X_{Ca}$  of garnet, yield temperatures of 335–430 °C, and 380–485 °C respectively.

Pressure was estimated utilizing the equilibrium curves  $Jd + Qtz = Ab$ , and  $Jd + Tlc = Gln$  (HOLLAND, 1980; MUIR WOOD, 1980). The jadeitic py-

roxene sliding equilibrium yields a minimum pressure in the absence of coexisting albite. For analyzed omphacites ( $Jd_{13-40}$ ), minimum pressures of 0.7–1.2 GPa at about 350–500 °C were obtained. A tentative P-T path is presented in figure 9. Note that although the Ti-rich phase parageneses observed in eclogitic rocks at Piampaludo are in topological agreement with the experimental phase diagram of figure 2 (LIU et al., 1996), inferred physical conditions are about 200 °C lower for the natural Fe+Ti-rich phase progression than for the laboratory synthesis fields for the MORB bulk composition. This disparity may reflect failure to achieve equilibrium in the laboratory experiments, or may represent the effect of differing Fe/Mg ratios of the MORB versus the Fe-Ti-rich Ligurian bulk chemistry.

The stable occurrence of talc with omphacitic pyroxene in eclogitic rocks indicates that metamorphism must have occurred at minimum pressures greater than the stability field of glaucophane. The end-member reaction defined by  $Gln = Jd + Tlc$  has been experimentally investigated by CARMAN and GILBERT (1983) and calculated by HOLLAND (1989). At 600 °C, the high-P assemblage jadeite + talc occurs at pressures greater than 3.0 GPa with a  $dP/dT$  slope of about 2.5 MPa per °C. This equilibrium curve, calculated by MUIR WOOD (1980) to pass through 400 °C at 1.75 GPa and 500 °C at 1.85 GPa, has been considered as the upper P limit for Italian high P/T metagabbros (POGNANTE and KIENAST, 1987). The P-T curve for the end-member reaction by HOLLAND (1989) is shown in figure 9. Using analyzed compositions of clinopyroxene ( $Jd_{40}$ ), talc, and sodic amphibole and the GEO-CALC program of BERMAN et al. (1987), we obtained a minimum pressure of 1.5 GPa at 400 °C. This value compares well with conditions determined by MESSIGA and SCAMBELLURI (1991) for crystallization of the Beigua eclogites: 1.3 GPa at 430 °C.

Tab. 9 Temperature estimates (°C) of rutile-bearing eclogites from Gruppo di Voltri, Italy.

| Sample    | $X_{Ca}$ | KD     | T1-1       | T1-2       | T2-1       | T2-2       |
|-----------|----------|--------|------------|------------|------------|------------|
|           |          |        | at 1.5 GPa | at 2.0 GPa | at 1.5 GPa | at 2.0 GPa |
| PR-8      | 0.079    | 28.775 | 353        | 363        | 450        | 475        |
|           | 0.176    | 59.808 | 326        | 335        | 367        | 389        |
| PR-24 (c) | 0.240    | 36.533 | 422        | 431        | 421        | 444        |
|           | (r)      | 0.146  | 26.712     | 404        | 414        | 459        |
| S2-15     | 0.212    | 64.412 | 338        | 346        | 360        | 382        |
|           | 0.116    | 38.631 | 340        | 350        | 414        | 438        |
| S2-116    | 0.184    | 38.629 | 380        | 389        | 414        | 438        |
| S3-42     | 0.138    | 49.058 | 326        | 335        | 388        | 410        |
|           | 0.138    | 37.693 | 356        | 365        | 417        | 441        |

T1, POWELL (1985); T2, RÄHEIM and GREEN (1974).

**Formation of titanite and the source of calcium**

Based on textural observations described in previous sections, we suggest the following conclusions: (1) titanite is not an eclogitic phase, and was

formed during retrogression under relatively low P-T conditions (only high F- and Al-bearing titanite might be an eclogite phase, as shown by CARSWELL et al., 1996); (2) several different reactions produce titanite; and (3) these processes oc-

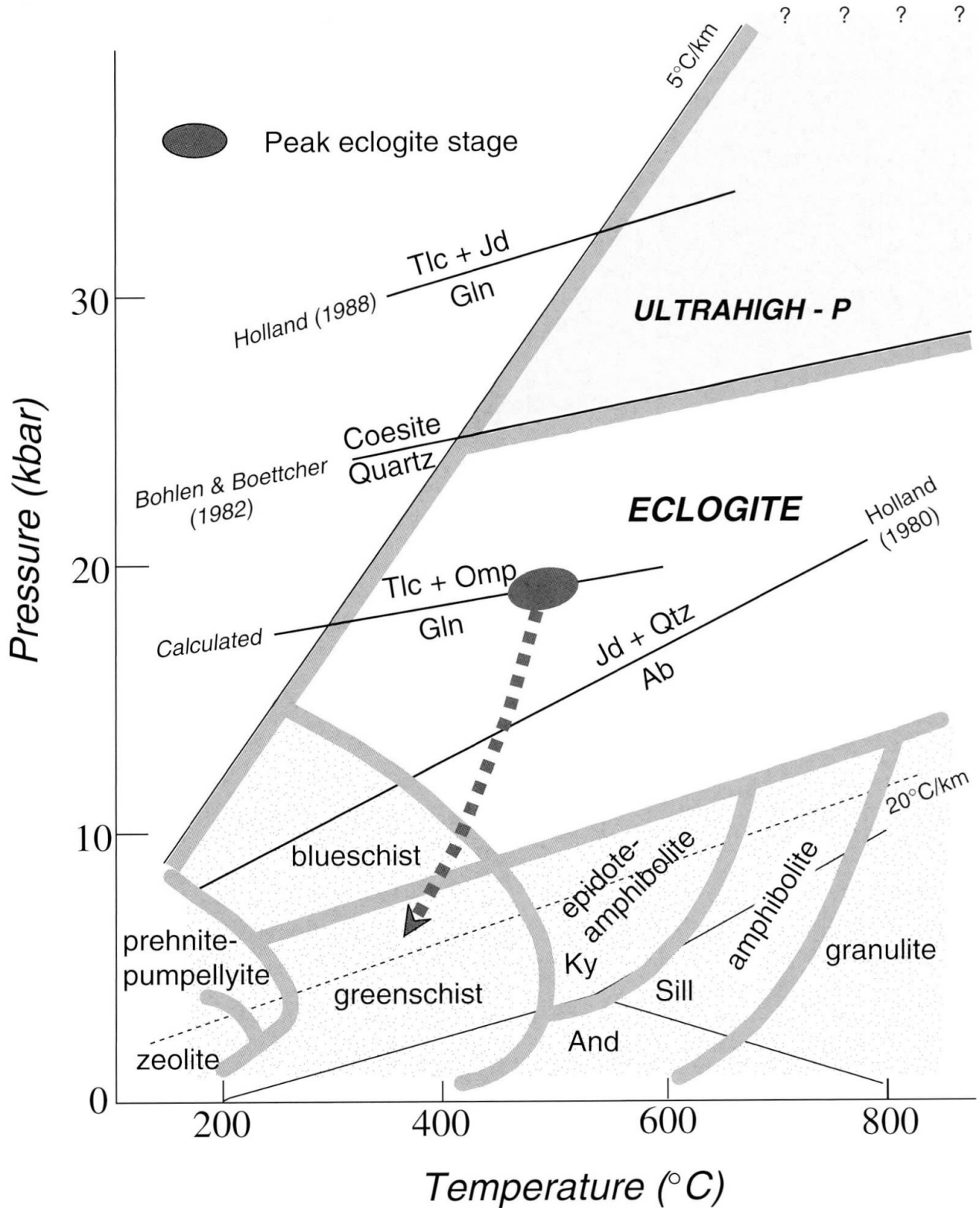
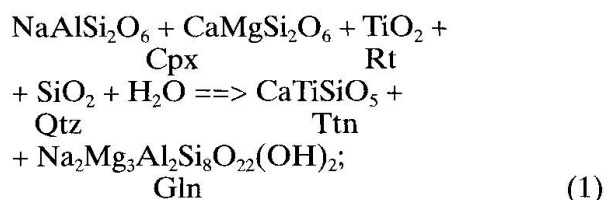


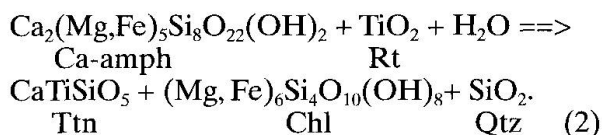
Fig. 9 P-T path showing the estimated peak conditions for eclogite-facies metamorphism and recrystallization during exhumation under blueschist- and greenschist-facies conditions, Gruppo di Voltri.

curred at different stages in the P-T evolution of these rocks.

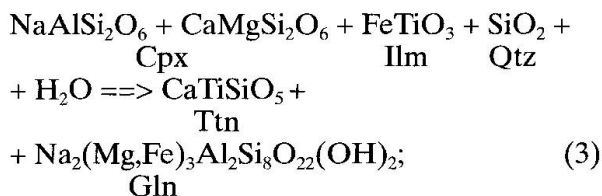
Titanite is closely associated spatially with rutile or ilmenite; the latter phases constitute the sources of Ti required for the formation of CaTiSiO<sub>5</sub>. Other associated phases are Na-amphibole, Ca-amphibole, epidote, chlorite, and quartz. Based on mineral and textural relationships, the following rutile-consuming reactions may be written:



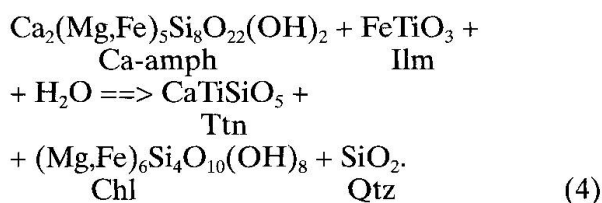
and



An additional pair of similar reactions was derived by substituting ilmenite for rutile in the above reactions:



and



These reactions clearly took place at different stages in the metamorphic evolution. Reactions (1) and (3) occurred at an early, higher pressure stage of the retrogression of amphibolite/blueschist-facies, and reactions (2) and (4) at later, lower pressure stages involving greenschist-facies conditions. Formation of titanite appears to have been continuous during retrograde metamorphism under amphibolite/blueschist- to greenschist-facies conditions. The source of calcium for titanite crystallization was the Ca-silicates associated with the Ti-bearing phases. Reactions (1) and (3) consume eclogitic omphacite, and reactions (2) and (4) consume secondary amphibole under low X<sub>CO<sub>2</sub></sub> conditions (e.g., ERNST, 1972). This suggestion is also consistent with the rare occurrence of carbonates in the investigated Italian samples.

### Metamorphic evolution

As described above, the Fe+Ti-rich gabbroic protolith contained plagioclase, augite, hornblende, titaniferous magnetite, Mn-rich ilmenite, and minor apatite as primary igneous phases. During high P/T eclogitic-facies metamorphism, plagioclase was transformed to Omp + Grt, augite to omphacite ± Na-amphibole, Fe-Ti oxide domains to Rt ± Grt, and Ti-bearing hornblende to rutile lamellae + katophorite. The typical mineral assemblage so produced was omphacite + Grt + Rt ± Tlc ± Qtz. During exhumation, these rocks underwent amphibolite/blueschist-, then greenschist-facies metamorphism. Eclogites were overprinted by a retrograde assemblage consisting of Grt + Gln ± barroisite + chloromelanite, then by the typical prasinitic association Act + Chl + Ab + Qtz ± Ep. The transition from eclogite to barroisitic amphibolite/blueschist appears to have been gradational; the same minerals occur in both assemblages and compositions of garnet and amphiboles appear to have continuously readjusted.

In spite of complicated metamorphic events, rutile is the dominant Ti-phase and subsequently was replaced by ilmenite and titanite accompanying amphibolite/blueschist-facies recrystallization at lower pressures. Eclogitization of Fe+Ti-rich gabbro evidently provides a unique natural process for the expulsion of Ti from oxides and high-Ti silicates and its concentration as rutile, reflecting the limited crystallochemical compliance of these phases in accommodating titanium at high pressures. Interestingly, ERNST and LIU (in press) have shown that the Ti content of hornblende is largely a function of temperature, and is practically insensitive to the pressure. Thus, high-T titaniferous hornblendes released TiO<sub>2</sub> to form rutile along amphibole cleavages during lower temperature eclogite facies recrystallization (e.g., Fig. 5A).

### Acknowledgements

Our project on the genesis of rutile ore in eclogitic rocks has been supported in part by E. I. du Pont de Nemours and Co., White Pigments and Mineral Products Unit, by NSF EAR 95-06468, and by the Stanford China Industrial Affiliates Program. Earlier petrographic and compositional data on minerals from Italian eclogites were collected by X. Wang and C.W. Oh. This manuscript has been critically reviewed by Felicity Lloyd, Eric Force, and Giovanni B. Picardo. We thank the above-named institutes and individuals for their support and assistance.

## References

- BERMAN, R.G., BROWN, T.H. and PERKINS, E.H. (1987): GEO-CALC: software for calculation and display of P-T-X phase diagrams. *Amer. Mineral.* 72, 861–862.
- BOHLEN, S.R. and BOETTCHER, A.L. (1982): The quartz-coesite transformation: a pressure determination and the effects of other components. *Jour. Geophys. Res.* 87, 7073–7078.
- BOHLEN, S.R. and LIOTTA, J.J. (1986): A barometer for garnet amphibolites and garnet granulites. *Jour. Petrol.* 27, 1025–1034.
- CARMAN, J.H. and GILBERT, M.C. (1983): Experimental studies on glaucophane stability. *Amer. Jour. Sci.* 283-A, 414–437.
- CARSWELL, D.A. (1990): Eclogites and the eclogite facies: definitions and classification. In: CARSWELL, D.S. (ed.): *Eclogite Facies Rocks*. Blackie Publishing Co., 1–13.
- CARSWELL, D.A., WILSON, R.N. and ZHAI, M. (1996): Ultrahigh pressure aluminous titanites in carbonate-bearing eclogites at Shuanghe in Dabieshan, central China. *Mineral. Mag.* 60, 461–471.
- CORTESOGNO, L., ERNST, W.G., GALLI, M., MESSIGA, B., PEDEMONTE, G.M. and PICCARDO, G.P. (1977): Chemical petrology of eclogitic lenses in serpentinite, Gruppo di Voltri, Ligurian Alps. *Jour. Geol.* 85, 255–277.
- ELLIS, D.J. and GREEN, D.H. (1979): An experimental study on the effect of Ca upon garnet-clinopyroxene Fe–Mg exchange equilibria. *Contr. Mineral. Petrol.* 71, 13–22.
- ERNST, W.G. (1972): CO<sub>2</sub>-poor composition of the fluid attending Franciscan and Sanbagawa low-grade metamorphism. *Geochim. Cosmochim. Acta*, 36, 497–504.
- ERNST, W.G. (1976): Mineral chemistry of eclogites and related rocks from the Voltri Group, western Liguria, Italy. *Schweiz. Mineral. Petrogr. Mitt.* 56, 293–343.
- ERNST, W.G. (1981): Petrogenesis of eclogites and peridotites from the Western and Ligurian Alps. *Amer. Mineral.* 66, 443–472.
- ERNST, W.G. and LIU, J. (in press): Experimental phase-equilibrium investigation of Al- and Ti-contents of clinopyroxene in oceanic tholeiite – a semiquantitative thermobarometer. *Amer. Mineral.*
- ESSENE, E., HENSON, B.J. and GREEN, D.H. (1970): Experimental study of amphibolite and eclogite stability. *Phys. Earth Planet. Interiors*, 3, 378–384.
- FORCE, E.R. (1991): Geology of titanium-mineral deposits. *Geol. Soc. Amer. Special Paper* 259, 112 pp.
- HELZ, R.T. (1973): Phase relations of basalts in their melting range at P<sub>H<sub>2</sub>O</sub> = 5 kb as a function of oxygen fugacity. *Jour. Petrol.* 14, 249–302.
- HELZ, R.T. (1979): Alkali exchange between hornblende and melt: a temperature-sensitive reaction. *Amer. Mineral.* 64, 953–965.
- HOLLAND, T.J.B. (1980): The reaction albite = jadeite + quartz determined experimentally in the range 600–1200 °C. *Amer. Mineral.*, 65, 129–134.
- HOLLAND, T.J.B. (1988): Preliminary phase relations involving glaucophane and applications to high pressure petrology: new heat capacity and thermodynamic data. *Contr. Mineral. Petrol.* 99, 134–142.
- HOLLAND, T.J.B. and POWELL, R. (1990): An enlarged and updated internally consistent thermodynamic dataset with uncertainties and correlations: the system K<sub>2</sub>O–Na<sub>2</sub>O–CaO–MgO–MnO–FeO–Fe<sub>2</sub>O<sub>3</sub>–Al<sub>2</sub>O<sub>3</sub>–TiO<sub>2</sub>–SiO<sub>2</sub>–C–H<sub>2</sub>–O<sub>2</sub>. *Jour. Metam. Geol.* 8, 89–124.
- HOOGERDUIN, S.E.H., RAMPONE, E., PICCARDO, G.B., DRURY, M.R. and VISSERS, R.L.M. (1993): Sub-solidus emplacement of mantle peridotites during incipient oceanic rifting and opening of the Mesozoic Tethys (Voltri Massif, NW Italy). *Jour. Petrol.* 34, 901–927.
- KRETZ, R. (1983): Symbols for rock-forming minerals. *Am. Mineral.* 68, 277–279.
- KROGH, E.J. (1988): The garnet-clinopyroxene Fe–Mg geothermometer – a reinterpretation of existing experimental data. *Contr. Mineral. Petrol.* 99, 44–48.
- LIOU, J.G., KUNIYOSHI, S. and ITO, K. (1974): Experimental studies of the phase relations between greenschist and amphibolite in a basaltic system. *Amer. Jour. Sci.* 274, 613–632.
- LIU, J., BOHLEN, S.R. and ERNST, W.G. (1996): Stability of hydrous phases in subducting oceanic crust: Earth Planet. Sci. Lett., 143, 161–171.
- MESSIGA, B., PICCARDO, G.B. and ERNST, W.G. (1983): High-pressure eo-Alpine parageneses developed in magnesian metagabbros, Gruppo di Voltri, Western Liguria, Italy. *Contr. Mineral. Petrol.* 83, 1–15.
- MESSIGA, B. and SCAMBELLURI, M. (1988): Comparison between two types of coronitic eclogites from the Western Alps: Implications for a pre-eclogitic evolution. *Schweiz. Mineral. Petrogr. Mitt.*, 68, 225–235.
- MESSIGA, B. and SCAMBELLURI, M. (1991): Retrograde P-T-t path for the Voltri Massif eclogites (Ligurian Alps, Italy): Some tectonic implications. *Jour. Metam. Geol.* 9, 93–109.
- MOODY, J.B., MEYER, D. and JENKINS, J.E. (1983): Experimental characterization of the greenschist/amphibolite boundary in mafic systems. *Amer. Jour. Sci.* 283, 48–92.
- MOTTANA, A. and BOCCHIO, R. (1975): Superferric eclogites of the Voltri group (Penninic belt, Apennines). *Contr. Mineral. Petrol.* 49, 201–210.
- MUIR WOOD, R. (1980): Compositional zoning in sodic amphiboles from the blueschist facies. *Mineral. Mag.* 43, 741–752.
- NEWTON, R.C. and SMITH, J.V. (1967): Investigations concerning the breakdown of albite at depth in the earth. *Jour. Geol.* 75, 268–286.
- POGNANTE, U. and KIENAST, J.R. (1987): Blueschist and eclogite transformations in Fe–Ti gabbros: A case from the western Alps Ophiolites. *Jour. Petrol.* 28, 271–292.
- POLI, S. (1993): The amphibolite-eclogite transformation: an experimental study on basalt. *Amer. Jour. Sci.* 293, 1061–1107.
- POLI, S. and SCHMIDT, M.W. (1997): The high-pressure stability of hydrous phases in orogenic belts: an experimental approach on eclogite-forming processes. *Tectonophysics* 273, 169–184.
- POWELL, R. (1985): Regression diagnostic and robust regression in geothermometer/ geobarometer calibration: the garnet-clinopyroxene geothermometer revisited. *Jour. Metam. Geol.* 3, 231–243.
- RÄHEIM, A. and GREEN, D.H. (1974): Experimental determination of the temperature and pressure dependence of the Fe–Mg partition coefficient for coexisting garnet and clinopyroxene. *Contr. Mineral. Petrol.* 48, 179–203.
- SCAMBELLURI, M., HOOGERDUIN, S.E.H., PICCARDO, G.B., VISSERS, R.L.M. and RAMPONE, E. (1991): Alpine olivine- and titanite-bearing assemblages in the Erro-Tobbio peridotite (Voltri Massif, NW Italy). *Jour. Metam. Geol.* 9, 79–91.
- SPEAR, F.S. (1981): An experimental study of hornblende stability and compositional variability in amphibolite. *Amer. Jour. Sci.* 281, 697–734.

- VALLIS, S. and SCAMBELLURI, M. (1996): Redistribution of high-pressure fluids during retrograde metamorphism of eclogite-facies rocks (Voltri Massif, Italian Western Alps). *Lithos* 39, 81–92.
- VISSERS, R.L.M., DRURY, M.R., HOOGERDUJN, S.E.H. and VAN DER WAL, D. (1991): Shear zones in the upper mantle: a case study in an Alpine lherzolite massif. *Geology* 19, 990–993.

Manuscript received September 1, 1998; revision accepted February 15, 1998.